Journal Pre-proofs

A sterilizable platform based on crosslinked xanthan gum for controlled-release of polymeric micelles: Ocular application for the delivery of neuroprotective compounds to the posterior eye segment

Sara Signorini, Andrea Delledonne, Silvia Pescina, Annalisa Bianchera, Cristina Sissa, Maria Vivero-Lopez, Carmen Alvarez-Lorenzo, Patrizia Santi, Cristina Padula, Sara Nicoli

PII: S0378-5173(24)00375-2
DOI: https://doi.org/10.1016/j.ijpharm.2024.124141
Reference: IJP 124141

To appear in: *International Journal of Pharmaceutics*

Received Date: 19 March 2024
Revised Date: 17 April 2024
Accepted Date: 18 April 2024

Please cite this article as: S. Signorini, A. Delledonne, S. Pescina, A. Bianchera, C. Sissa, M. Vivero-Lopez, C. Alvarez-Lorenzo, P. Santi, C. Padula, S. Nicoli, A sterilizable platform based on crosslinked xanthan gum for controlled-release of polymeric micelles: Ocular application for the delivery of neuroprotective compounds to the posterior eye segment, *International Journal of Pharmaceutics* (2024), doi: https://doi.org/10.1016/j.ijpharm.2024.124141

~~**Controlling the release of polymeric micelles with a sterilizable xanthan gum—based platform for drug delivery to the posterior eye segment**~~

A sterilizable platform based on crosslinked xanthan gum for controlled-release of polymeric micelles: ocular application for the delivery of neuroprotective compounds to the posterior eye segment

Sara Signorini[a], Andrea Delledonne[b], Silvia Pescina[a], Annalisa Bianchera[a], Cristina Sissa[b], Maria Vivero-Lopez[c], Carmen Alvarez-Lorenzo[c], Patrizia Santi[a], Cristina Padula[a], Sara Nicoli[a]*

[a] ADDRes Lab, Department of Food and Drug, University of Parma, Parco Area delle Scienze 27/a, 43124 Parma, Italy.

[b] Department of Chemistry, Life Science and Environmental Sustainability, University of Parma, Parco Area delle Scienze 17/a, 43124 Parma, Italy.

[c] Departamento de Farmacología, Farmacia y Tecnología Farmacéutica, I+D Farma (GI-1645), Facultad de Farmacia, Instituto de Materiales (iMATUS) and Health Research Insititute of Santiago de Compostela (IDIS), Universidade de Santiago de Compostela, 15782 Santiago de Compostela, Spain.

Sara Signorini[a]	sara.signorini@unipr.it
Andrea Delledonne[b]	andrea.delledonne@unipr.it
Silvia Pescina[a]	silvia.pescina@unipr.it
Annalisa Bianchera[a]	annalisa.bianchera@unipr.it
Cristina Sissa[b]	cristina.sissa@unipr.it
Maria Vivero-Lopez[c]	maria.vivero@nottingham.ac.uk
Carmen Alvarez-Lorenzo[c]	carmen.alvarez.lorenzo@usc.es
Patrizia Santi[a]	patrizia.santi@unipr.it
Cristina Padula[a]	cristina.padula@unipr.it
Sara Nicoli[a]*	sara.nicoli@unipr.it

Corresponding author:
Sara Nicoli PhD
Department of Food and Drug,
Parco Area delle Scienze, 27/A
University of Parma
43124 Parma, Italy
Tel. +39 0521 905065/71
E-mail: sara.nicoli@unipr.it
ORCID ID: https://orcid.org/0000-0001-6955-0957

Abstract

TPGS (D-α-tocopheryl polyethylene glycol 1000 succinate) polymeric micelles show interesting properties for ocular administration thanks to their solubilization capability, nanometric size and tissue penetration ability. However, micelles formulations are generally characterized by low viscosity, poor adhesion and very short retention time at the administration site. Therefore, the idea behind this work is the preparation and characterization of a crosslinked film based on xanthan gum that contains TPGS micelles and is capable of controlling their release. The system was loaded with melatonin and cyclosporin A, neuroprotective compounds to be delivered to the posterior eye segment. Citric acid and heating at different times and temperatures were exploited as crosslinking approach, giving the possibility to tune swelling, micelles release and drug release. The biocompatibility of the platform was confirmed by HET-CAM assay. ***Ex vivo*** studies on isolated porcine ocular tissues, conducted using Franz cells and two-photon microscopy, demonstrated the potential of the xanthan gum-based platform and enlightened micelles penetration mechanism. Finally, the sterilization step was approached, and a process to simultaneously crosslink and sterilize the platform was developed.

Keywords

Xanthan gum, ocular drug delivery, polymeric film, TPGS micelles, sterilization, crosslinking

Funding statement

This work has been carried out in the frame of the ALIFAR project, funded by the Italian Ministry of University and Research through the program 'Dipartimenti di Eccellenza 2023-2027'.
SS benefited of a PhD fellowship financed under the National Recovery and Resilience Plan (NRRP), Mission 4 Component 1 Investment 3.4 and 4.1 - Call for tender No. 351 of 09/04/2022 of Italian Ministry of University and Research funded by the European Union – NextGenerationEU.
AD and CS have benefited from the equipment and framework of the COMP-HUB and COMP-R Initiatives, funded by the 'Departments of Excellence' program of the Italian Ministry for University and Research (MIUR, 2018-2022 and MUR, 2023-2027).
This work has received funding from the European Union's Horizon 2020 research and innovation programme under the Marie Skłodowka-Curie grant agreement No 101007804 (Micro4Nano).
AD acknowledge the support of the Italian Ministry for University and Research (MUR) through the project Efficient Light Harvesting with Self-assembled Peptide Nanostructures (LANTERN), 20225NPY8P, within the National Recovery and Resilience Plan (NRRP) PRIN2022 action.
CAL has received support from the AEI/10.13039/501100011033 [PID 2020-113881RB-I00].

1. Introduction

Retinal diseases such as age-related macular degeneration (AMD), diabetic retinopathy and glaucoma account for the majority of irreversible blindness cases worldwide (Health Organization, n.d.). The treatment of these diseases is very problematic, since, at the moment, there are limited – if any – therapeutic tools. While diabetic retinopathy and wet-AMD are controlled with corticosteroids and anti-vascular endothelial growth factor (anti-VEGF) compounds, dry-AMD cannot be treated. Glaucoma as well cannot be cured and it is only managed by lowering intraocular pressure. Despite presenting multiple and different pathogenic mechanisms, often not entirely clear, these pathologies have as common outcome the oxidative stress and the apoptosis of different retinal cells (Pardue and Allen, 2018; J. Wang et al., 2022). Several evidences suggest that neuroprotective compounds could contribute to preserve the patient's current visual function promoting neuronal survival (Pardue and Allen, 2018), but their administration still represents a challenge. Indeed, the delivery of actives to the retina is very difficult due to numerous static and dynamic barriers that protect the inner structures of the eye (Nayak and Misra, 2018). For this reason, drugs – when available – are typically administered by intravitreal injections. This invasive route is associated with poor patient compliance and side effects, aggravated by the high administration frequency required for chronic pathologies (Thrimawithana et al., 2011). Therefore, an effective and less invasive administration strategy for targeting the posterior eye segment represents one of the most relevant medical needs in the ophthalmology field (Gabai et al., 2023) and is an essential requirement in case of adjuvant and preventive treatments.

In recent decades, nanometer-sized systems have attracted great interest for ocular delivery (Madni et al., 2017; Qi et al., 2023) and, among them, polymeric micelles have emerged as a promising carrier for the delivery of hydrophobic compounds (Ghezzi et al., 2021). Polymeric micelles (10-200 nm) are based on amphiphilic molecules capable of self-assembling into organized core-shell/supramolecular structures in aqueous media at concentrations exceeding their critical micellar concentrations (CMC). These nanocarriers consist of an inner lipophilic core, which is involved in the loading of hydrophobic compounds, and an outer hydrophilic shell facing the aqueous medium, which is responsible for the interaction of the micelles with the environment (Figure 1, Panel A). Their capability for overcoming ocular barriers and improving the delivery of lipophilic drugs to the anterior and posterior eye segments has recently been highlighted (Durgun et al., 2020; Vaneev et al., 2021). Among other suitable amphiphilic polymers, micelles made of D-α-tocopheryl polyethylene glycol 1000 succinate (TPGS) gave notable results (Ghezzi et al., 2022; X. Li et al., 2021; Pescina et al., 2021; Rathod et al., 2021). TPGS is a biocompatible and biodegradable non-ionic surfactant, formed by the esterification reaction between vitamin E succinate and polyethylene glycol, and capable of self-assembling into micelles of about 13 nm in size. Previous studies have demonstrated permeation-enhancing activity in cornea and conjunctiva (Duan et al., 2015; Lu et al., 2024; Ostacolo et al., 2013; Pescina et al., 2021, 2019; Terreni et al., 2021b, 2020), the capability to diffuse intact within the scleral tissue and to control drug release through esterase-mediated TPGS hydrolysis (Ghezzi et al., 2022; Grimaudo et al., 2018).

Despite the permeation enhancement results – which could support the development of less invasive administration methods – TPGS micellar solutions are characterized by low viscosity and poor adhesion, which reflect in a short residence time at the application site and, in perspective, in the need for frequent administrations. Frequent administrations reduce adherence to the treatment and cause fluctuations in drug tissues concentration with possible side effects.

Therefore, the idea behind this work was the preparation and characterization of a polymeric platform, in the form of a film, that contains micelles (Figure 1, Panel B) and is capable of controlling their release after ocular administration. The drug-loaded micelles, once slowly released from the platform, can take advantage of their nanometric size, solubilization capability and tissue penetration to enhance drug delivery to the ocular tissues. A further objective of the work was to prepare this platform using biocompatible and sustainable materials, through an easy and scalable preparation process, also paying attention on the sterilization step, a key process for all ocular formulations.

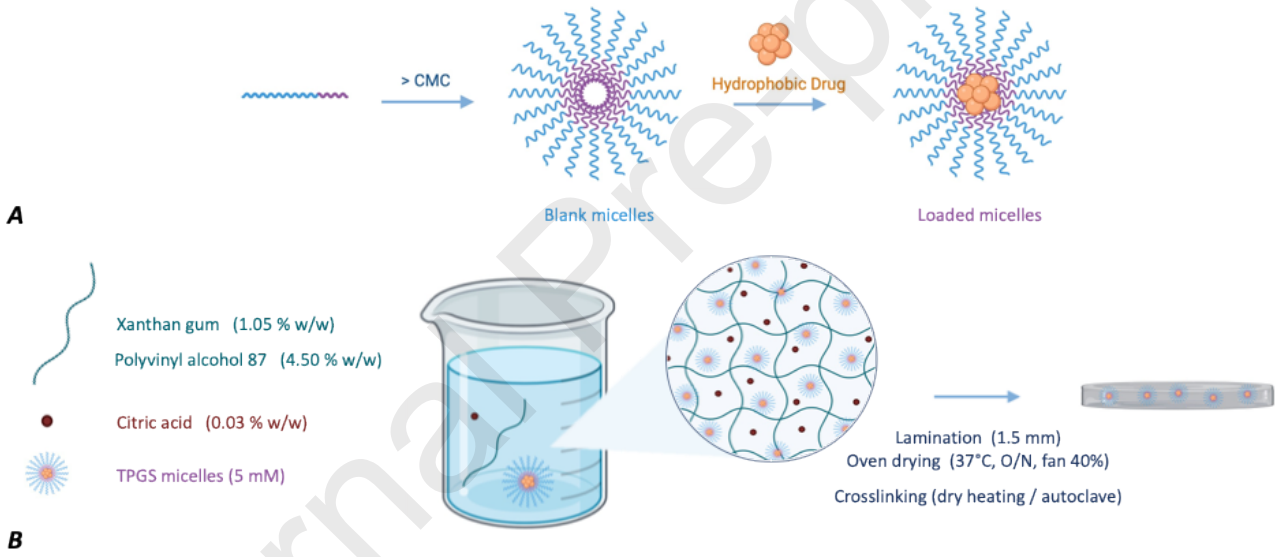

Figure 1. Structure and formulation of micelles (Panel A); TPGS micelles loading into the platform/film for their controlled release (Panel B).

This work relied on the hypothesis that xantham gum (XG), a safe anionic polysaccharide used in swelling-controlled drug release formulations (Chandra et al., 2022; Cortes et al., 2020; Pahuja et al., 2012), can regulate the diffusion of the micelles towards the ocular surface if the pore size of the hydrogel network is adequately tuned. XG is composed of a β-(1→4)-D-glucopyranose glucan backbone with side chains of (1→3)-α-D-mannopyranose-(2→1)-β-D-glucuronic acid-(4→1)-β-D-mannopyranose on alternating residues. Compared to other anionic polysaccharides, the branched structure of XG makes it advantageous in terms of mucoadhesivess and structural agent since the conformation of its chains, and thus the viscosity, is less dependent on changes of solvents, temperature or pH (Nsengiyumva and Alexandridis, 2022). Moreover its biotechnological origin confers XG production more eco-sustainable. The film forming capability of XG was reinforced by adding polyvinyl alcohol (PVA), which forms transparent, thin and easily handled films (Cascone et

al., 1995; Kodavaty, 2022). XG and PVA have already been associated in a variety of fields, from the food area to the pharmaceutical one, resulting in a promising basis for the preparation of drug delivery systems (Bhattacharya et al., 2012; Bhunia et al., 2013; Brunchi et al., 2016; Ray et al., 2010). TPGS was used for the preparation of the micelles and citric acid (CA) was chosen as the crosslinking agent, to control micelles release. The hydrophobic compounds cyclosporine A (CYC) and melatonin (MEL) were selected as neuroprotective agents to be loaded into the micelles. MEL and several of its metabolites act as free radical scavengers and efficient antioxidants (Hardeland and Pandi-Perumal, 2005; Lundmark et al., 2007; Yu et al., 2021); it also has anti-inflammatory and immunomodulation activity, contributing to the protection of the retinal tissue (Diéguez et al., 2020; Ferreira de Melo et al., 2020; Sande et al., 2014). CYC is widely effective in the treatment of ocular inflammatory states and is also reported to promote retinal ganglion cell survival (Kim et al., 2014). Both MEL and CYC proved to be protective against both hypoxia and glutamate-induced neuronal cell damage (Ruiz et al., 2000; Schnichels et al., 2021; C. Wang et al., 2022; Zhang et al., 2023).

After the definition of film composition, the crosslinking conditions (heating time and temperature) were studied and optimized to control the swelling properties and thus tune the release of the micelles. The ocular biocompatibility was evaluated by HET-CAM assay, while ***ex vivo*** studies on isolated ocular tissues were carried out using diffusion cells and two-photon microscopy to confirm the potential of the formulated platform and gain an insight into the penetration mechanism of micelles. Finally, the sterilization step was addressed, and a process was developed to simultaneously crosslink and sterilize the platform.

2. Experimental section

2.1 Materials

Polyvinyl alcohol (PVA, MW 83,400 Da; hydrolysis degree 86.5 – 89.0 mol %) was purchased from Gohsei (Osaka, Japan). Xanthan gum from *Xanthomonas campestris* (XG, MW 2,000 – 20,000 kDa; 1 % solution Brookfield viscosity 915 cPs; 50 % terminal mannose residues were 4,6-pyruvated while most of the inner mannose residues were 6-acetylated), melatonin (MEL, MW 232.28 g/mol; LogP 1.6) and Nile red (NR, 9-(diethylamino)-5H-benzo[a]6henoxazine-5-one; MW 318.4 g/mol) were purchased from Sigma-Aldrich (St. Louis, MO, USA). Tocopheryl polyethylene glycol 1000 succinate (TPGS) was a kind gift from PMC ISOCHEM (Vert-Le-Petit, France). Citric acid (CA) was purchased from A.C.E.F. S.p.a (Fiorenzuola d'Arda, Italy), while cyclosporine A (CYC, MW 1202.6 g/mol; LogP 3 (El Tayar et al., 1993)) was from Alfa Aesar (Haverhill, MA, USA).

Purified water (Purelab Pulse, Elga Veolia, UK) was used; acetonitrile and methanol were of HPLC grade, while trifluoroacetic acid (TFA) and all other reagents were of analytical grade. Phosphate buffer saline (PBS) had the following composition: 0.19 g/L KH_2PO_4, 2.37 g/L Na_2HPO_4, 8.8 g/L NaCl and was adjusted to pH 7.4 with H_3PO_4. Acetate buffer was prepared by dissolving in water 1.48 g/L $C_2H_3O_2Na$ and mixing with acetic acid 4.67 mL/L; pH was adjusted to 4.8 using 1 M NaOH.

For microbiological assays, Mueller Hinton Broth and Sabouraud (Oxoid Ltd., Basingstoke, Hants, UK) were used as liquid mediums, while Tryptic Soy Agar (Scharlab, Barcelona, Spain) was used as a solid medium. Mueller Hinton Broth medium was prepared by dissolving 21 g of the commercial formulation (typical formula, modified to meet performance standards: beef, dehydrated infusion from 300.0 g/L; casein hydrolysate 17.5 g/L; starch 1.5 g/L; pH 7.3 $\pm$ 0.1 at 25 °C; divalent cation content of the lot: 4.473 mg/L Ca^{2+} and 7.067 mg/L Mg^{2+}) in 1 L of pure water. Sabouraud liquid medium was prepared by dissolving 30 g of the commercial formulation (typical formula: pancreatic digest of casein 5.0 g/L; peptic digest of fresh meat 5.0 g/L; glucose 20.0 g/L; pH 5.7 $\pm$ 0.2 at 25 °C) in 1 L of pure water. Tryptic Soy Agar was prepared by dissolving 40 g of the commercial formulation (general purpose medium containing animal and plant peptone, according to Pharmacopoeial Harmonized Methods and ISO standards) in 1 L of pure water (typical formula: casein peptone 15 g/L; soy peptone 5 g/L; sodium chloride 5 g/L; agar 15 g/L; pH 7.3 $\pm$ 0.2 at 25 °C). All the media were sterilized by autoclave at 121 °C for 15 minutes.

2.2 HPLC-UV quantification methods

Analyses were performed under isocratic conditions using an HPLC-UV system (Infinity 1260, Agilent Technologies, Santa Clara, CA, USA). TPGS and CYC analytical methods were previously published (Ghezzi et al., 2022; Pescina et al., 2019), while the analytical method for MEL was adapted starting from the method developed by Martins et al. (Martins et al., 2017). Details on the HPLC-UV methods used for the different compounds are reported in Table 1, while the validation parameters are presented in the Supplementary Material section (Table S1). The two methods reported for the quantification of CYC are interchangeable.

Table 1. HPLC-UV methods for the different analytes.

PARAMETER	TPGS (Ghezzi et al., 2022)	CYCLOSPORINE A (Ghezzi et al., 2022) , (Pescina et al., 2019)		MELATONIN
COLUMN	Symmetry300 C18, 250 × 4.6 mm, 5 µm (Waters, Milford, MA, USA)	Aeris Widepore XB-C8, 150 x 4.6 mm, 3.6 µm (Phenomenex, Torrance, CA, USA)	Nova-Pak C18, 150 x 3.9 mm, 4 µm Cartridge (Waters, Milford, MA, USA)	Atlantis dC18, 150 x 3.9 mm, 3 µm (Waters, Milford, MA, USA)
GUARD COLUMN	SecurityGuard Widepore C18 (Phenomenex, Torrance, CA, USA)	-	SecurityGuard Widepore C18 (Phenomenex, Torrance, CA, USA)	SecurityGuard Widepore C18 (Phenomenex, Torrance, CA, USA)
OVEN TEMPERATURE (°C)	40	65		32
MOBILE PHASE	pH 4.8 acetate buffer : CH_3OH (3:97 v/v)	CH_3CN : water with 0.1 % TFA (55:45 v/v)	CH_3CN : water with 0.1 % TFA (65:35 v/v)	CH_3CN : water (35:65 v/v)
FLOW (mL/min)	2	1.6		1
INJECTION VOLUME (µL)	100	100		20
ABSORPTION WAVELENGTH (nm)	215	230		220
RETENTION TIME (min)	~ 4	~ 5	~ 6.5	~ 2.8

2.3 Polymeric film formulation and crosslinking

2.3.1 Film preparation

For film preparation, a 5 mM (0.76 % w/v) TPGS micellar solution was firstly prepared by simple dissolution of the polymer in ultrapure water. This solution was added either with XG to obtain a 1.5 % w/w solution, or with PVA to obtain a 15 % w/w solution. The XG and PVA solutions were then mixed in a 70/30 weight ratio and CA was added as crosslinking agent at a final concentration of 0.03 % w/w. The obtained homogeneous gel was centrifuged three times at 3,000 rpm for 5 minutes to remove entrapped air bubbles. It was then laminated with a film casting knife (BYK Gardner, Silversprings, MD, USA) at a thickness of 1.5 mm on the non-functionalized side of a fluorinated liner (9956 Release Medical Liner, Polyester, Fluoropolymer, 3M) fixed on a glass plate. Drying was performed in an air-circulating oven (Model FED 056, BINDER GmbH, Germany) at 37 °C (fan 40 %) overnight. For simplicity, the formulation obtained under these conditions is indicated as *Formulation A*. Table 2 reports the theoretical composition of the mixture and the dry film, calculated assuming the total elimination of water after drying.

To study the mechanism of crosslinking, films without CA (*Formulation B* in Table 2), without XG and without both XG and TPGS were also prepared. However, the presence of TPGS proved to be essential to obtain a formulation with good qualitative properties.

Table 2. Composition % (w/w) of *Formulation A* and *Formulation B*, before and after drying (assuming the total elimination of water).

COMPONENT	*Formulation A*		*Formulation B*	
	WET FORMULATION	DRY FORMULATION	WET FORMULATION	DRY FORMULATION
	Composition (% w/w)		Composition (% w/w)	
PVA	4.50	71.09	4.50	71.43
XG	1.05	16.59	1.05	16.67
TPGS	0.75	11.85	0.75	11.90
CA	0.03	0.47	–	–
H_2O	93.67	–	93.70	–

2.3.2 Crosslinking using dry heating

High temperatures were used as a strategy to crosslink the films. Pieces (6x6 cm size) of the films were placed on a glass plate and introduced in an oven pre-set to the desired temperature (121 or 130 °C; fan 40 %). Heating duration was 19 minutes in case of 121 °C and 19, 30, 60 and 90 minutes in case of 130 °C. Additional 5 minutes were required to reach the set temperature after placing the film in the oven.

To evaluate the role of all film components in the crosslinking process, CA-free films (*Formulation B*) and XG-free films were also subjected to the treatment. Table S2 in Supporting Information summarizes the different conditions evaluated.

2.3.3 Crosslinking using moist heat (autoclave)

As a potential platform for ophthalmic use, the possibility of crosslinking the formulation in a contextual way to autoclave sterilization was evaluated. For this purpose, sections (6x6 cm size) of the films (*Formulations A* and *B)* were placed in an autoclave (CertoClav Sterilizer GmbH, Leonding, Austria) using a heat-sealed aluminum bag as a support (raw aluminum, primed and with heat sealant – Lamp Pharmaceuticals, S. Prospero, Modena, Italy). The crosslinking/sterilization process took place at a fixed temperature (121 °C). In the case of *Formulation A* the time was 15 minutes, while, in the case of *Formulation B*, various times were evaluated, namely 15, 16, 17, 18, 20, 25 and 30 minutes. Beyond the sterilization time, approximately 8 additional minutes were necessary to reach the useful pressure and, at the end of the process, 1 minute to recover the sample.

2.3.4 Drug-loaded films

Melatonin and cyclosporine A were included in the film after their solubilization in TPGS micelles. Briefly, a 2.2 mg/mL MEL solution in 5 mM TPGS was prepared by adding the required amount of drug to the micellar solution and by stirring (400 rpm) at room temperature for about one hour. In the case of cyclosporine A, a 0.8 mg/mL CYC solution in 5 mM TPGS was prepared by adding 1 mL of CYC solution in 95° ethanol (concentration 20 mg/mL) to 25 mL of 5 mM TPGS. The system was left to stir overnight at room temperature to favor the evaporation of the ethanol and the integration of the drug into the micelles.

Size and polydispersity index (PDI) of the drug-loaded micelles were measured by Dynamic Light Scattering (DLS) using a Zetasizer Nano-ZSP (Malvern Instruments, Malvern, UK). For comparison, also unloaded 5 mM TPGS micelles were analyzed. Measurements were performed at 25 °C after filtration of the solutions (regenerated cellulose 0.45 μm filters).

The drug-loaded micellar solutions obtained were then used for the preparation of the polymeric films, as described in section 2.3.1. Film composition is reported in Table S3. Film crosslinking was performed both at 121 °C for 19 minutes and at 130 °C for 90 minutes (dry heating).

2.4 Characterization of the polymeric films

2.4.1 Appearance, thickness and weight

The appearance of the films was visually evaluated and their thickness and weight were measured. Thickness was determined using a digital thickness gauge (Absolute Digimatic, Mitutoyo, Milan, Italy; model ID-C112BS; serial n.o. 02101, 0.001-12.7 mm), at a temperature of about 25 °C and relative humidity equal to 64 ± 8 %. The films were then sampled with a 0.28 cm^2 area and weighed to obtain the weight/cm^2.

2.4.2 Mechanical properties

Mechanical properties of dried films (strips of 3x1 cm) were recorded in a TA.XT Plus Texture Analyzer (Stable Micro Systems, Ltd., Surrey, UK) fitted with a 5 kg load cell. The films were fixed to the lower and the upper mini-clamps (15 mm gap) and subjected to uniaxial stress at 0.1 mm/s. The Young's modulus was calculated from the slope of the linear portion of the engineered stress versus engineered strain curves.

2.4.3 Swelling studies

Swelling studies were conducted on blank film samples of 0.28 cm^2 area. 5 mL of saline solution (NaCl 0.9 % w/v; pH 5.79 $\pm$ 0.14) were pipetted into a vial into which the thin films, previously weighted (m_0), were individually dipped without stirring. At specific time points, each film was removed from the solution, swabbed lightly with filter paper and accurately weighed (m_t). The swelling index S_I was calculated using Equation 1, where m_0 is the weight of the dry film, and a graph of S_I versus time was plotted. The procedure was performed in triplicate, at room temperature.

$$S_I = \frac{m_t - m_0}{m_0}$$ Equation 1

2.4.4 SEM analysis

Blank samples (area 0.6 cm^2) of *Formulation A*, crosslinked in an oven at 121 °C for 19 minutes and 130 °C for 90 minutes were placed in contact with 100 μL of 0.9 % w/v NaCl solution for 60 minutes. After this time, the swollen films were subjected to freeze-drying (see Table S4 for freeze-drying conditions). SEM images of the surface and cross-sectional area were recorded in a Zeiss EVO LS15 Scanning Electron Microscope (Oberkochen, Germany). The samples were not previously treated and the images were collected working at 20 kV, using a backscattered electron detector (BSD detector) and under variable pressure (VP) conditions.

2.4.5 Microbiological assay

Formulation B crosslinked in the autoclave at 121 °C for 18 minutes was subjected to a microbiological test to confirm effective sterilization: samples of 0.28 cm^2 area were placed in the solid and liquid media described in section 2.1. In the case of the solid medium, samples were deposited with the addition of 100 μL of sterilized 0.9 % (w/v) NaCl saline solution. All the samples were incubated at 37 °C for 10 days. For each medium, the evaluation was performed in triplicate, with a negative and a positive control.

2.4.6 TPGS and drug content in the films

To quantify the amount of TPGS, cyclosporine A or melatonin in the prepared films, samples with an area of either 0.28 (TPGS and MEL) or 0.6 (CYC) cm^2 were deposited in a glass vial containing 5 mL of 0.9 % w/v NaCl solution and left to stir vigorously until complete disgregation/solubilization. The time required for the non-crosslinked formulation was about 1 hour and increased for the crosslinked formulations. The longest stirring time was approximately 13 hours, required for the crosslinked formulation under the most severe conditions (130 °C – 90 minutes). The obtained solution was sampled, filtered (regenerated cellulose 0.45 μm filters) or centrifuged (13,000 rpm for 15 minutes) and, after suitable dilution with the same solvent, analyzed by HPLC-UV with the method described in Table 1. Despite the poor solubility of CYC, the simultaneous release of the drug with TPGS increased its solubility in NaCl (0.9 % w/v) saline solution. The determination was carried out in triplicate, at room temperature. The data collected were then reported as a percentage of the expected theoretical value. The same procedure was followed to determine the stability of the drugs in the formulations after 8 months of storage (room temperature, 64 ± 8 % relative humidity, protected from light).

2.4.7 Release of TPGS and drugs from the prepared films

Samples with an area of either 0.28 (TPGS and MEL) or 0.6 (CYC) cm^2, homogeneous in thickness and weight, were placed in glass vials containing 5 mL of 0.9 % w/v NaCl solution kept under slow magnetic stirring (80 rpm). The solution was sampled (300 μL) at defined times, refilling with fresh

solution to restore the initial volume. The samples were then analyzed by HPLC-UV (Table 1). The study was carried out in triplicate, at room temperature.

2.5 HET-CAM test

Fertilized hen's eggs (50-60 g; Coren, Spain) were used to perform irritation tests on the chorioallantoic membrane (CAM) as previously reported (Vivero-Lopez et al., 2022). The HET-CAM assay is not considered an animal experiment under Directive 2010/63/EU as no nervous system is developed before embryonal day (ED) 11 (European Parliament and Council, 2010). The chick chorioallantoic membrane is not innervated, and the Institutional Animal Care and Use Committee (IACUC) and the USA National Institutes of Health established that a chick embryo does not experience pain until ED 14 and is not considered as a living animal until ED17 (Kundeková et al., 2021). 26 eggs were incubated in a climatic chamber (Ineltec, model CC SR 0150, Barcelona, Spain) at 37 °C and 60 % relative humidity for 8 days, with regular turning (3 times per day) until the day before the test when they were placed with the wider extreme upward. Then, the eggshell above the air chamber was partially detached (1 cm in diameter) and the inner membrane was wetted with 0.9 % w/v NaCl for 30 minutes before being carefully removed to expose the CAM. The unloaded and CYC-loaded formulations (area 0.28 cm^2), crosslinked and uncrosslinked, were placed on the CAM, in duplicate. 0.9 % w/v NaCl and 0.1 M NaOH solutions (300 μL) were used as negative and positive controls, respectively. The vessels of the membrane were observed for 5 minutes, recording the times at which hemorrhage (Th, vessels bleeding), vascular lysis (Tl, vessels disintegration), or coagulation (Tc, denaturalization of intra- and extra-vascular proteins) occurred. The irritation score (IS) was calculated using the Equation 2.

$$IS = \left(\frac{301-Th}{300} \times 5\right) + \left(\frac{301-Tl}{300} \times 7\right) + \left(\frac{301-Tc}{300} \times 9\right) \quad \text{Equation 2}$$

2.6 *Ex vivo* studies

2.6.1 Tissues preparation

Fresh porcine eyes, by-products of meat processing for human consumption, were supplied by a local slaughterhouse (Macello Annoni S.p.A., Parma, Italy). Eye bulbs were isolated, after the death of the animal, from Landrace and Large White animals (females and males, age 10-11 months, weight 145-190 kg) and maintained in PBS at 4 °C until their use in the experiments, which occurred within 2 hours from the enucleation.

For the experiment across conjunctiva, the tissue was isolated from the lower part of the eyeball and, still attached to the eyeball, was mounted on the diffusion cell (section 2.6.2). For scleral retention and permeation, the muscular and connective tissues around the eye bulb were completely removed. The isolated sclera was obtained by circumferentially cutting and removal of the anterior segment of the eye behind the limbus. The collected eyecup was then cut and everted. The neural retina and the choroid-Bruch's layer were discarded, while the sclera was used for the permeation experiments (section 2.6.3). For the experiments across the choroid, after the isolation of the posterior segment of the eye, the neural retina was eliminated and the RPE, weakly fixed to

the Bruch's membrane, was easily detached by applying filter paper. After the removal of the whole RPE, the choroid-Bruch's membrane was detached using tweezers, cutting the vessels engaged in the sclera with a scalpel, and mounted on diffusion cells (section 2.6.4).

2.6.2 Retention and permeation experiments across the conjunctiva

The experiments were performed using 0.2 cm^2 Franz-type diffusion cells (DISA, Milano, Italy). The tissue, still attached to the eyeball, was applied to the lower compartment with the stromal side facing the receptor compartment, taking care to avoid stretching of the tissues. The donor compartment was then applied, the system was clamped, and the eyeball was carefully removed by cutting the external conjunctiva with scissors (Pescina et al., 2019). After cell assembly, the receptor compartment was filled with approximately 4 mL of degassed 0.9 % w/v NaCl solution (saline). The cell was placed in a thermostatic bath at 37 °C and the receptor solution was stirred magnetically, to avoid any boundary layer effects. A sample of 0.13 cm^2 area of the crosslinked (121 °C for 19 minutes) polymer formulation loaded with CYC (section 2.3.4) was placed into the donor compartment on which 150 μL of saline solution were deposited. The donor and receptor compartments were covered with parafilm. At the end of the experiment (5 hours), the receptor fluid was sampled and analyzed. The solution remaining in the donor was withdrawn, the formulation was removed, the conjunctiva was washed (saline solution, 1 mL) and dried with filter paper. The donor washing solution with the film was then diluted to 5 mL with water, placed under stirring until complete solubilization, filtered (regenerated cellulose 0.45 μm filters) and then analyzed by HPLC-UV (Table 1). TPGS and CYC retained in the tissue were extracted overnight with 1 mL of the extraction mixture (CH_3CN: 1%CH_3COOH, 87:13 v/v). Extraction solutions were filtered with 0.45 μm regenerated cellulose filters (Phenomenex, Torrance, CA, USA) before HPLC-UV analysis (Table 1). The extraction procedures were previously validated for cyclosporine A (Grimaudo et al., 2018) and confirmed in their ability to extract also TPGS (Ghezzi et al., 2022). Each condition was replicated 8 times.

2.6.3 Retention and permeation experiments across the sclera

The experiments were performed using glass Franz-type diffusion cells (DISA, Milano, Italy) with a permeation area of 0.6 cm^2. After the proper filling of the receiving compartment (section 2.6.2), a 0.6 cm^2 area sample of the crosslinked polymer formulation (121 °C for 19 minutes) loaded with CYC (section 2.3.4) was placed in the donor compartment with 150 μL of saline solution. The donor and receptor compartments were covered with parafilm, placed in a thermostatic bath (37 °C) and the receptor solution was stirred magnetically, to avoid any boundary layer effects. The duration of the experiment was 24 hours. At the end of the experiment, the receptor solution was sampled and analyzed, the solution remaining in the donor was withdrawn, the formulation was removed and weighed, the tissue was washed (saline, 5 mL) and dried with filter paper. CYC and TPGS were extracted by treating tissues with 1 mL solution of CH_3CN: 1%CH_3COOH, 87:13 (v/v). Samples were left under these conditions overnight at room temperature, then sonicated for 12 minutes and centrifuged at 12,000 rpm for 15 minutes before HPLC-UV analysis (Ghezzi et al., 2022; Grimaudo et al., 2018). Experiments were replicated 8 times.

2.6.4 Permeation experiments across choroid

The isolated choroid was mounted on Franz-type diffusion cells (0.2 cm^2 area) with the scleral side facing the donor compartment and without any type of support (Pescina et al., 2012). The cell was mounted and placed as described in section 2.6.2 and the duration of the experiment was 5 hours. 150 μL of a 5 mM TPGS solution loaded with CYC (section 2.3.4) were applied into the donor compartment. Donor and receptor were covered with parafilm. Every 30 minutes, the receptor solution was sampled for the determination of permeated TPGS and CYC. The flux (J, μg/cm^2h) was calculated as the slope of the regression line in the condition of steady-state, while the apparent permeability coefficient (P, cm/s) was calculated as J/Cd where Cd (μg/mL) represents the concentration of the donor solution. At the end of the experiment, the solution remaining in the donor was withdrawn, the tissue was washed (saline, 2 mL) and dried with filter paper. Experiments were replicated 4 times.

2.7 TPGS hydrolysis in contact with the conjunctiva

The ***in vitro*** enzymatic hydrolysis of TPGS was evaluated using conjunctiva from fresh porcine eyes. In particular, the isolated tissue (section 2.6.1) was biopsied to obtain a sample of approximately 60 mg. A 100 μg/mL solution of TPGS was prepared by dissolving the polymer in a mixture of PBS pH 7.4: water in a ratio 1:10. Then, 300 μL of TPGS 100 μg/mL were incubated with the biopsied tissue for 24 hours at 37 °C. At predetermined time intervals, samples were centrifuged at 12,500 rpm for 5 minutes and 40 μL of the TPGS solution were withdrawn and diluted 1:10 with CH_3CN: 1%CH_3COOH 87:13 (v/v), causing esterase inactivation. The concentration of TPGS in these samples was measured by HPLC-UV. Control samples obtained in the same conditions but without tissue were analyzed as well.

2.8 Two-photon microscopy

Nile red (NR) – loaded TPGS 5 mM micelles were prepared to add a fluorescence functionality to polymeric micelles, so that they can be probed by two-photon microscopy. Briefly, 4 μL of a 1 mg/mL NR solution in DMSO were added to 1 mL of blank 5 mM TPGS micelles, resulting in a 4 μg/mL NR solution. The micellar solution was used for the preparation of the film. After crosslinking (121 °C – 19 minutes), 0.28 cm^2 samples were used in ***ex vivo*** studies on conjunctiva (2h application) and sclera (4h application). The tissues were mounted on Franz-type cells (0.6 cm^2) (sections 2.6.2 and 2.6.3). The same experiments were also performed using unloaded films.

Films and ocular tissues were analyzed with a Two-Photon Microscope Nikon A1R MP+ Upright equipped with a femtosecond pulsed laser Coherent Chameleon Discovery (~ 100 fs pulse duration with 80 MHz repetition rate). Sample were excited at 820nm. A 25× water dipping objective with a numerical aperture of 1.1 and 2-mm working distance was employed for focusing the excitation light and for collecting the two-photon excited fluorescence (TPEF) and the second harmonic generation (SHG) signals. TPEF/SHG signal was detected by three non-descanned high sensitivity GaAsP photomultiplier tubes preceded by optical filters allowing the simultaneous acquisition of

three separated channels: blue channel (415 – 485 nm), green channel (506 – 593 nm) and red channel (604 – 679 nm). Imaging overlay of the three channels and processing was performed by the operation software of the microscope. Additionally, the spectral profiles have been recorded with a fourth GaAsP photomultiplier detector, connected to the microscope through an optical fiber and preceded by a dispersive element (wavelength range 430 to 650 nm with a bandpass of 10 nm).

For microscope observations, performed right after dismounting the tissue from the Franz-type cell, the samples were placed in a dedicated plexiglass holder and saline solution was used to dip the objective and to avoid dehydration. Excitation wavelength was set at 820 nm to collect both images and spectra. Images were acquired with a field of view of 500 µm × 500 µm.

2.9 Statistical analysis

All data presented in text, figures and tables are reported as mean value ± SD. For sake of clarity, mean value ± SEM (standard error of the mean) was used in the case of permeation experiment across choroid. The significance of the differences between the results was assessed using Student's t-test. Differences were considered statistically significant when $p < 0.05$.

3. Results and discussion

3.1 Formulation

TPGS has been widely investigated as excipient for the development of liquid and semisolid formulations, thanks to its potential as solubilizing agent, emulsifier, stabilizer and permeation enhancer (Guo et al., 2013; Mehata et al., 2023; Yang et al., 2018). However, the use of TPGS in the preparation of polymeric films is far less explored. TPGS can act as a plasticizing agent to enhance the mechanical properties of films made of hydrophilic polymers such as hydroxypropyl cellulose (Repka and McGinity, 2001), pullulan (Vuddanda et al., 2017) or chitosan (Bi et al., 2020), or lipophilic polymers, namely poly(L-lactic) and poly(lactic-co-glycolic) acid (Dong et al., 2008). Also TPGS can block efflux pumps to increase the bioavailability of drugs administered as films (Malathi et al., 2020). Terreni and colleagues (Terreni et al., 2021a) investigated the use of mixed micelles containing octylphenoxy poly(ethyleneoxy) ethanol and TPGS in mucoadhesive inserts. In the present paper, we used TPGS as a micelle-forming polymer to load hydrophobic compounds in a XG hydrophilic film. Once released from the crosslinked film, micelles can promote drug penetration across ocular tissues and TPGS hydrolysis can contribute to the antioxidant activity.

The film was easily prepared by hydration of XG and PVA in a TPGS micellar solution (micelle size: 13 nm), addition of the crosslinking agent (CA), lamination at 1.5 mm thickness and drying overnight at 37 °C. The composition of the mixture and the theoretical composition of the polymeric film are shown in Table 2 (*Formulation A*). A film without citric acid (*Formulation B*) was also prepared. Film thickness and weight were 69.3 ± 0.58 µm and 8.50 ± 0.27 mg/cm^2, respectively. A representative picture of the film is depicted in Figure S1 in Supporting Information.

3.2 Crosslinking of polymeric films and their characterization

Uncrosslinked films completely dissolved in less than one hour; thus, crosslinking was needed to preserve film structure and control the release of the micelles over time. Combination of CA and temperature has been shown as a non-hazardous, ecofriendly way to crosslinking polymers rich in hydroxyl groups, such as polysaccharides and PVA, by forming ester bonds (Diaz-Gomez et al., 2022; Shijie Xu et al., 2022). In the present study, different temperatures (121 and 130 °C) and crosslinking times (19, 30, 60 and 90 minutes) were evaluated. The procedure did not substantially affect neither the thickness nor the weight of the films (Table S5).

3.2.1 Swelling studies

The crosslinking effect was initially investigated by recording the swelling index (S_I) as a function of time. For films crosslinked at 130 °C, as the treatment time increased, the S_I decreased (Figure 2, Panel A). The film crosslinked for only 19 minutes allowed a more gradual swelling compared to longer crosslinking times. When the temperature was reduced to 121 °C (19 minutes), higher and faster swelling was recorded, with a water uptake of 37.20 ± 3.96 % after 210 minutes. All crosslinked films remained intact for at least 5 days in 0.9 % (w/v) NaCl.

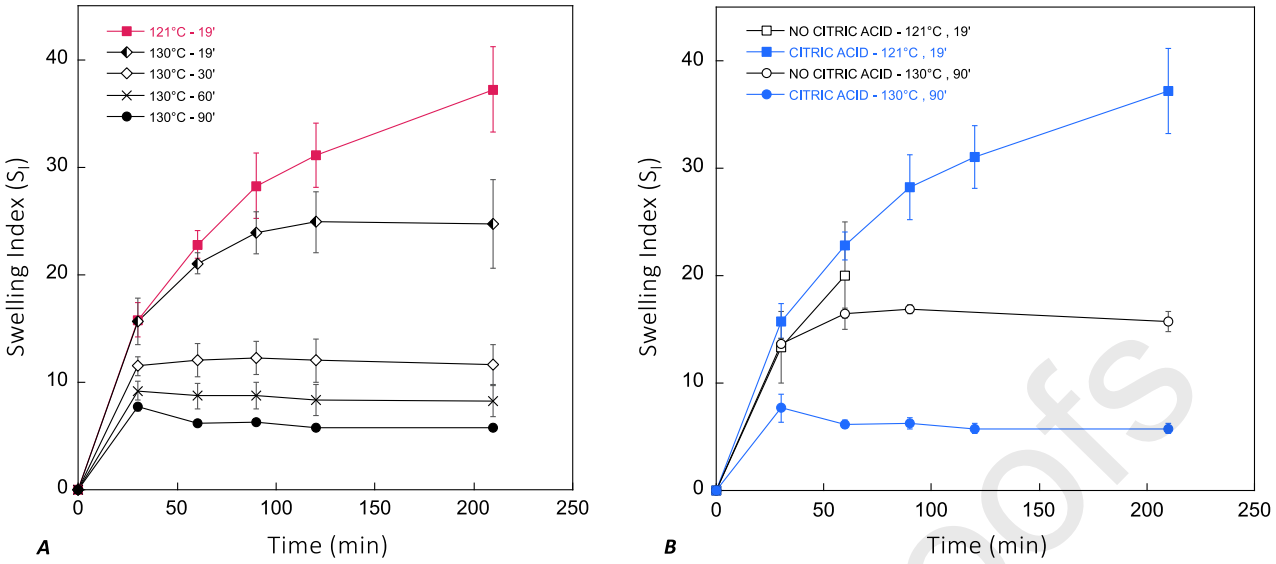

Figure 2. Film swelling in 0.9 % (w/v) NaCl . Panel A: effect of crosslinking time and temperature (dry heating) on the swelling properties of the film containing CA (*Formulation A*). Panel B: effect of the crosslinking agent CA on the swelling index of crosslinked films under different conditions (dry heating). The curve of the formulation without CA (*Formulation B*) crosslinked 121 °C - 19' stoped at 60 minutes because the film disintegrated. All data are reported as mean ± SD (n = 3).

After this preliminary evaluation, the harshest (130 °C for 90 minutes) and the mildest (121 °C for 19 minutes) conditions were selected to investigate the role of each component in crosslinking. Films prepared without XG (Table S2) dissolved within 5 minutes even when submitted to the harshest conditions, suggesting that, despite its lower proportion in the film (16 % w/w), XG is the only polymer responsible for the formation of the network. Literature data indicate that PVA can be crosslinked as well in the presence of CA (do Nascimento et al., 2021; Gautam et al., 2022), but probably it needs higher temperatures, higher CA concentration, a catalyzer and/or longer times.

The role of CA is illustrated in Figure 2, Panel B. In milder conditions and without CA (*Formulation B* in Table 2), the film dissolved between 60 and 90 minutes, while under the most drastic conditions, the film preserved its structure for some hours even without adding CA, although it underwent a more significant swelling than when CA was incorporated. Literature data confirm the ability of XG to crosslink (Bueno et al., 2013; Reddy and Yang, 2010). In the presence of CA, a condensation process, which involves dehydration and the formation of ester bonds between CA and the polymer chains, takes place. In the absence of CA, if the temperature is high enough, the acidic groups of XG (pyruvilic or acetyl) interact with the hydroxyl groups forming intra- and intermolecular ester bonds (dehydration and transesterification reactions).

3.2.2 Release of TPGS from the film

Once the role of crosslinking in the swelling process was clarified, we tried to understand how this reflected on the release kinetics of the TPGS micelles, selecting again the harshest and the mildest conditions of the dry heating crosslinking process that are referred from now on as “130 °C” and “121 °C”, respectively. This was possible after confirming the compound stability: TPGS in the

uncrosslinked film was 99.7 ± 2.3 % of the theoretical value; after crosslinking, the percentage was 92.9 ± 3.2 % and 86.6 ± 7.4 % at 121 °C and 130 °C respectively. The heating procedure caused a slight decrease in the TPGS content although, due to the high variability, the data were not significantly different (p = 0.25). These results suggest that TPGS was not involved - or maybe minimally involved - in covalent bonds formation during the crosslinking process.

Release studies performed on non-crosslinked film showed that TPGS was completely released within the first hour (data not shown), while crosslinked films controlled the release of TPGS (Figure 3, Panel A). However, unexpectedly, the harsher crosslinking condition was associated with a faster TPGS release (90 % released in 3 hours), while the milder one controlled the release up to 25 hours (percentage released was 91.76 ± 0.32 %).

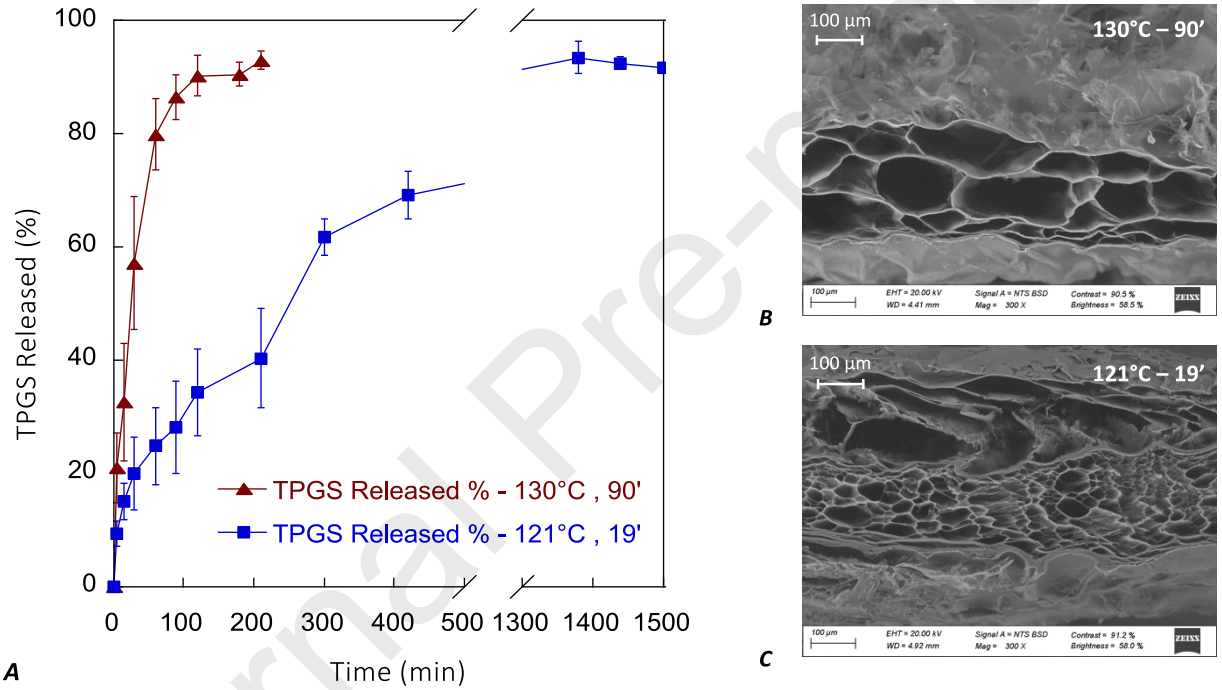

Figure 3. Panel A: comparison between the release of TPGS in 0.9 % w/v NaCl saline solution from the selected dry heating crosslinked (121 °C for 19 minutes and 130 °C for 90 minutes) films (*Formulation A*). Data are reported as mean ± SD (n = 3). Panels B and C: SEM images of the cross-section of swollen films (*Formulation A*) crosslinked at 130 °C for 90 minutes (Panel B) and at 121 °C for 19 minutes (Panel C). Scale bar 100 µm.

To shed light on this behavior, the swelled films were subjected to freeze-drying and then analyzed by SEM (Figure 3, B and C). The film crosslinked at 130 °C had larger and less numerous pores (Figure 3, Panel B) than the film crosslinked at 121 °C (Figure 3, Panel C). Lien et al. obtained a similar result when crosslinking gelatin scaffolds: the pore size of the scaffold increased as the crosslinking temperature raised. Authors attributed this behavior to a different reaction rate: at higher temperatures bonds are formed instantly leading to larger pores while lower temperatures favor greater interaction between the polymer chains and therefore the formation of smaller meshes (Lien et al., 2009).

The three-dimensional characteristics of the systems could contribute **to explaining** the TPGS release kinetic. Despite the size of the meshes are in both cases much bigger than the micelles' size (see Table 3), the slower release recorded for the system crosslinked at 121 °C could be due to the more tortuous path that the micelles must face during their diffusion. The different tortuosity of the meshes found in the cross-sections is also confirmed in the different organization of the surfaces of the swollen samples (Figure S2 in Supporting Information).

3.3 Loading of neuroprotective compounds

The oxidative stress that characterizes neurodegenerative eye diseases causes progressive damage to the optic nerve and to specialized retinal cells. The administration of neuroprotective compounds can help to stop, decrease or even inhibit some of the steps by which the radical species generate the death of retinal cells (Pardue and Allen, 2018). Among all these compounds, melatonin (MEL) and cyclosporine A (CYC) were singled out. Both molecules are poorly water-soluble, therefore TPGS micelles could increase both their solubility and the transport across the ocular barriers (Ghezzi et al., 2022). Films loaded with the drug-containing micelles could act as a platform for the sustained supply of the therapeutic agents to the ocular tissues.

3.3.1 Drug-loaded films

MEL and CYC were first solubilized in a 5 mM TPGS solution before being loaded into the film. The characteristics of the micellar solutions and the concentration of the drugs in the final formulation are summarized in Table 3. DLS data showed that blank micelles had very small dimensions (average of about 13 nm) and that the loading of the drugs did not change their sizes.

Table 3. Dimensional characteristics of blank and loaded micellar solutions and drug concentration in the final film. All the micellar formulations were limpid.

	DRUG CONCENTRATION IN THE 5 mM MICELLAR SOLUTION (mg/mL)	MICELLES SIZE (nm) and POLIDISPERSITY INDEX (PDI)	THEORETICAL DRUG CONCENTRATION IN THE FILM (w/w %)	THEORETICAL DRUG CONCENTRATION IN THE FILM (μg/cm²)
BLANK	-	13.5 ± 4.1 (0.085)	-	-
MEL	2.2 *	12.7 ± 3.7 (0.211)	3.15	268
CYC	0.8 **	13.0 ± 4.2 (0.149)	1.17	99

* MEL solubility in water is 1.6 mg/mL; MEL solubility in 5 mM TPGS is 2.5 mg/mL.

** CYC solubility in aqueous solution is about 0.035 mg/mL; CYC solubility in 5 mM TPGS is 1 mg/mL.

After loading, MEL concentration in the dry film was 3.15 % w/w, corresponding to 268 μg/cm^2, while CYC concentration in the dry film was 1.17 % w/w, corresponding to 99 μg/cm^2. Furthermore,

the loading of the drugs and the subsequent crosslinking did not significantly modify the thickness and weight/cm^2 of the loaded films compared to the unloaded ones (Table S5).

The exact composition of each film (Table S3) and the stability of the active compounds during the crosslinking procedure (Table S6) are reported in Supporting Information. MEL and CYC stability in the films was also evaluated after 8 months of storage at room temperature and, also in this case, the % remaining was close to 100 % of the t = 0 value (Table S6).

Drug release studies were performed on the crosslinked formulations at 121 °C and 130 °C (Figure 4). The release of the active compounds from the film depended both on the release of TPGS micelles and on the percentage of drug actually loaded into the micelles.

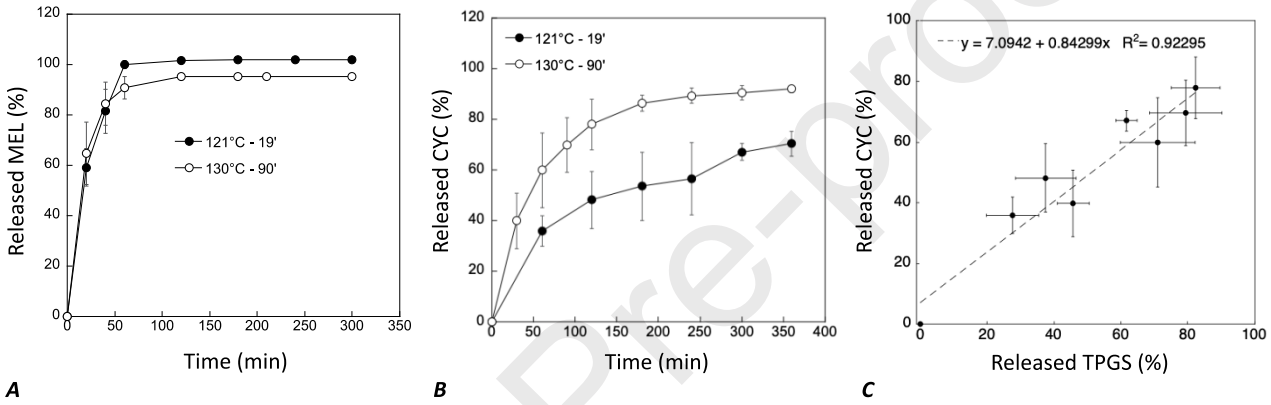

Figure 4. Release of MEL (Panel A) and CYC (Panel B) in 0.9 % w/v NaCl saline solution as medium from crosslinked films (*Formulation A*) at 130 °C and 121 °C. Panel C illustrates the relation between the % of CYC released and the % of TPGS released. Data are reported as mean ± SD (n = 3).

In fact, MEL dose was almost entirely released within the first hour (Figure 4, Panel A), with a much faster release rate than TPGS. Furthermore, the crosslinking condition did not influence MEL release kinetics. The data can be justified by assuming that MEL was poorly loaded inside the micelles, but it was mainly dissolved as free molecules in the polymeric network. This hypothesis is supported by the moderate difference in MEL solubility between water (1.6 mg/mL) and 5 mM TPGS solution (2.5 mg/mL). A small molecule not included in the micelles can diffuse more rapidly in the hydrated film, which is therefore unable to control its release.

Unlike melatonin, CYC was efficiently loaded in the TPGS micelles (solubility in water < 0.05 mg/mL; solubility in 5mM TPGS = 1 mg/mL), and it could be released following the diffusion of the micelles through the polymeric network. Indeed, when the percentage of CYC released was plotted as a function of the percentage of TPGS released (Figure 4, Panel C) a linear correlation with a slope reasonably close to 1 was found.

Considering the absence of control in drug release, it was decided to stop the studies on MEL-loaded films, while only the platform loaded with CYC was selected for subsequent evaluations. In addition,

only the milder crosslinking condition was studied on ocular tissues, since it represents the best option to control CYC release from the film (Figure 4, Panel B).

3.4 *Ex vivo* studies on ocular tissues: permeation studies and two-photon microscopy

The ocular absorption of drugs is prevented by numerous static, dynamic, and metabolic barriers (Cholkar et al., 2013). The static barriers to the retina are represented by the conjunctiva, the sclera and the bilayer choroid-Bruch's membrane. In principle the platform could be applied in the conjunctival sac (non-invasive application of an ocular insert), with the conjunctiva as the first obstacle, or on the scleral surface (subconjunctival implant) (Figure 5). In the latter case, the loaded micelles avoid the conjunctiva but should still cross the sclera and the choroid-Bruch's membrane to reach the retinal pigment epithelium (RPE), the pigmented layer of the retina.

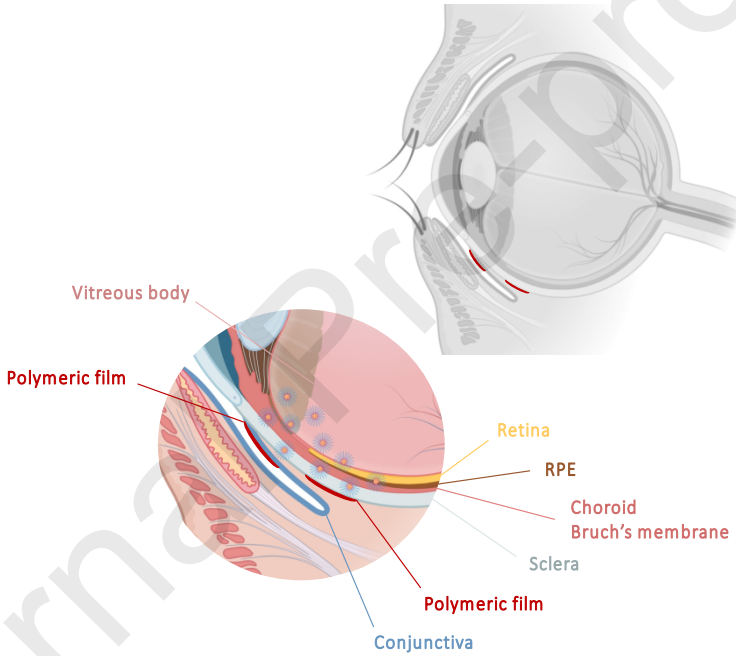

Figure 5. Schematic representation of film application in the conjunctival sac or as a sub-conjunctival implant and illustration of the main ocular barriers (thickness of the different tissues is not to scale). Created with BioRender.com.

Ex vivo experiments were performed with both CYC-loaded films crosslinked at 121 °C and with Nile red (NR)-loaded films prepared in the same conditions (section 2.3.4). The emissive features of NR-loaded films were first investigated by two-photon microscopy (TPM).

3.4.1 Two-photon microscopy analysis of the films

Blank and NR-loaded films were analysed by two-photon microscopy (TPM) and the images obtained by irradiating the samples at 820 nm are shown in Figure 6. Blank and NR-loaded films showed weak green and intense red fluorescence, respectively. As shown in Figure S3, the emission

detected in blank films is mainly due to XG, that is likely to be fluorescent thanks to the residual impurities derived from the production and manufacturing processes.

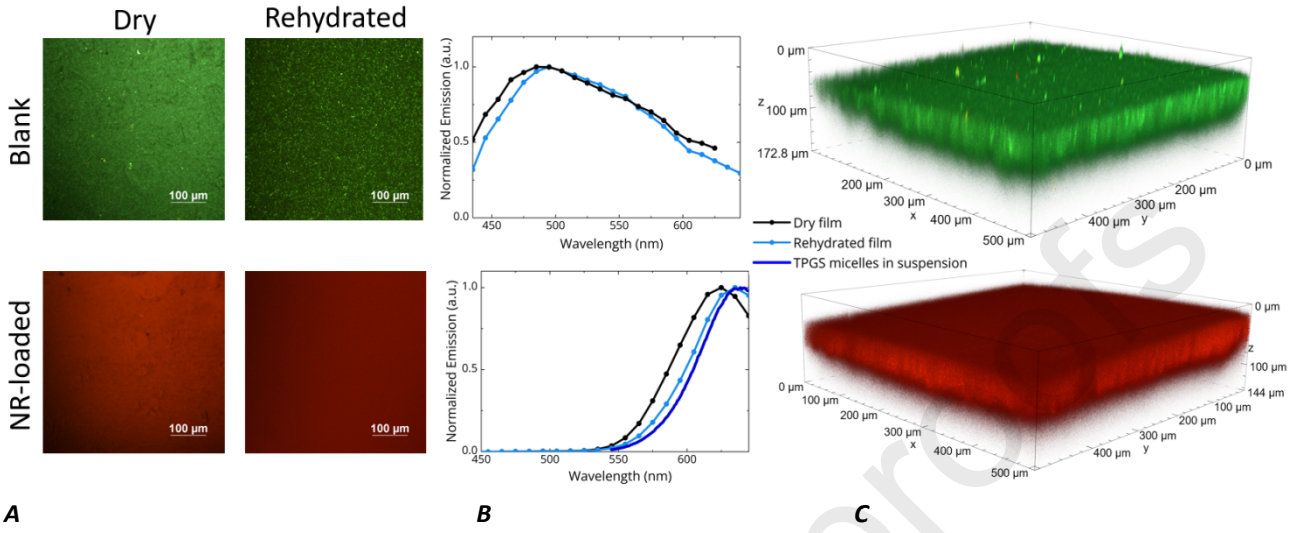

Figure 6. Two-photon microscopy images (Panel A), normalized emission spectra (Panel B) and volume renderings reconstructed from Z-stacks (Panel C, Z-step: 1.1 µm, total depth: 173 or 144 µm) acquired from blank (top panels) and NR-loaded (bottom panels) films irradiating the sample at 820 nm. The measurements in panels A and B were performed both before and after rehydration with NaCl saline solution (0.9 % w/v), while the renderings in panel C refer to dry films. Images and spectra of films loaded with NR were acquired using a reduce laser power with respect to blank samples, in order to avoid saturation of detectors.

NR is a solvatochromic probe (Boldrini et al., 2002), thus its emission spectrum changes with the polarity of the environment. For this reason, to further investigate the emissive features of the films, emission spectra, both before and after the rehydration process, were recorded (Figure 6, Panel B). In the case of the blank films, two emission peaks (495 and 585 nm) with slightly variable relative intensity were observed. The emission profile of the NR-loaded film was subjected to a slight red-shift after the rehydration process, suggestive of an increase in the polarity of the environment of the dye (emission peak after rehydration: 635 nm) in the presence of water. This emission spectrum almost overlapped the emission spectrum recorded on the NR-loaded micellar solution (Ghezzi et al., 2022), confirming TPGS reassembly into micelles after film rehydration (Figure 6, Panel B). No significant differences were observed in the emission of the crosslinked and uncrosslinked polymeric films (see Figure S4 for the corresponding measurements on uncrosslinked films).

3.4.2 Retention and permeation studies across the conjunctiva

The non-invasive procedure to target the retina would involve the application of the formulation in the conjunctival sac. From here, the drug/nanocarrier should diffuse through the conjunctival-scleral route (Figure 5), which is considered the easiest way to the posterior segment (Grimaudo et al., 2019). Many researchers are investigating this possibility, even if, at the moment, the data do not allow to draw conclusive results on the clinical feasibility of this approach (Rodrigues et al., 2018).

In view of this possible application, the film was applied to the conjunctiva for 5 hours and both CYC and TPGS were quantified in the tissue and in the receptor compartment.

The amount of CYC retained in the conjunctiva was 5.22 ± 0.90 μg/cm^2, while TPGS accumulation in the tissue was equal to 12.75 ± 10.09 μg/cm^2. The TPGS/CYC ratio in the tissue was 2.4, much lower compared to the one present in the micelles and in the film (9.5). This can be attributable to two different phenomena: 1) cyclosporine-loaded micelles does not penetrate intact into the tissue and disassemble in contact with the epithelial cells; 2) TPGS can be metabolized inside the conjunctiva. To investigate these two aspects, metabolism studies and TPM studies were performed. Figure 7, Panel A illustrates TPGS degradation in contact with the conjunctival mucosa and highlights the high metabolic activity of the tissue, apparently higher in comparison with the previously studied cornea and sclera (Ghezzi et al., 2022; Grimaudo et al., 2018).

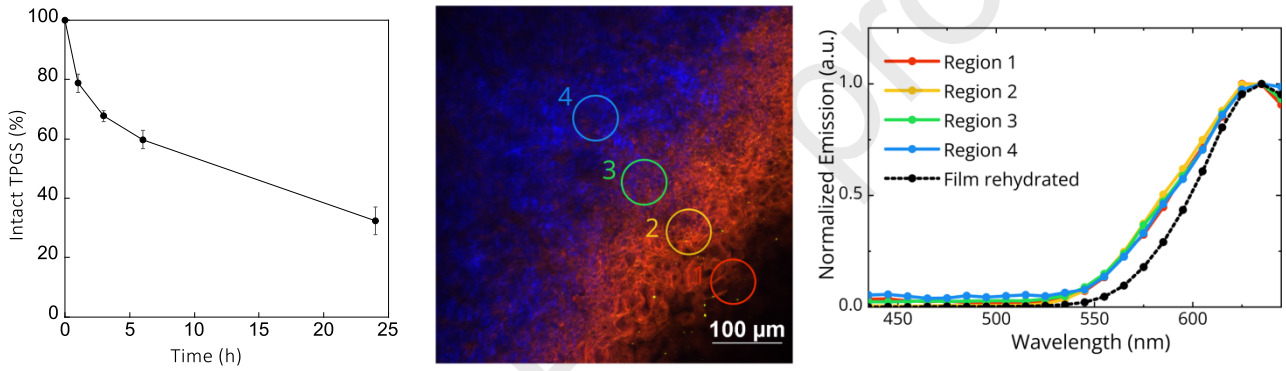

A ***B*** ***C***

Figure 7. Panel A: percentage of intact TPGS recovered after contact with conjunctiva at 37 °C. The ratio between TPGS amount (30 μg) and conjunctival tissue (60 mg) was around 0.5 μg/mg of tissue. The data is the mean value of 6 samples from 6 different eyes (mean ± SD). Panel B: TPM image of conjunctiva treated with a NR-loaded film, placed during the experiment in contact with the epithelium of Region 1. A more complete and detailed view of the 3D conjunctiva treated with a NR-loaded film is available in Supplementary Movie S1. Panel C: normalized emission spectra collected from four different circular regions of the image reported in Panel B. The emission profile of a rehydrated film is reported as a comparison. Both images and emission spectra were acquired at 820 nm.

Figure 7 shows an image (Panel B) and four emission spectra collected from the conjunctiva treated with the NR-loaded film (Panel C) for 2 hours. The epithelial cells, whose volume progressively decreases while going deeper into the inner layers (from Region 1 to 4), were clearly highlighted by the presence of NR which accumulated in their cytoplasm and cell membranes. Blue color refers to the conjunctival stroma where the collagen fibers are responsible for the second-harmonic generation (SHG) signal (Ghezzi et al., 2022) (a more complete and detailed view of the 3D conjunctiva treated with a NR-loaded film is available in Supplementary Movie S1). In order to better understand the micelles behavior, emission spectra from the tissue were acquired. In fact, emission spectrum of NR changes with the polarity of the environment (Boldrini et al., 2002) and this, in principle, could differentiate between NR in the micelles core and NR released in the tissue. Emission profiles collected from conjunctiva at different depths (Figure 7C) had a peak at 635 nm and did not

show a sizable shift as observed in the case of corneal epithelium (Ghezzi et al., 2022). This suggests that micelles can penetrate intact in the tissue, thanks to the lower barrier properties of the conjunctiva, characterized by fewer desmosomes between the epithelial cells if compared to the cornea (John V. Forrester et al., 2016; Polisetti et al., 2023). However, the signal was clearly broadened in the low-wavelength region, and this can be attributed to a partial NR release in a less polar environment, such as the cell membranes. It is worth mentioning that XG emission and tissue autofluorescence could have partially contributed to this result, even if the signal present in the samples treated with blank films is much lower and variable (see Figure S5, that presents images and emission spectra acquired from conjunctiva treated with the blank film). An animated 3D view of the conjunctiva treated with the blank film is available in Supplementary Movie S2.

Concerning permeation experiments, despite the thinness of the conjunctiva and its limited barrier properties, after 5 hours no drug was found in the receptor compartment, while the presence of TPGS was detected but quantification was not possible (< LOQ). These results highlight that the conjunctival application of the film to target the retina is not feasible: the extremely fast metabolism of TPGS in contact with this tissue is not counterbalanced by the slow micelle release from the system. However, this formulation could be interesting for the treatment of dry eye disease (where the conjunctiva itself represents the target). As a consequence of TPGS metabolism, the release of vitamin E and vitamin E succinate, both antioxidant compounds, could have a positive effect on the treatment of this disease (L. Li et al., 2021; Mccusker et al., 2016; Wong, 2009).

3.4.3 Permeation and retention studies across sclera and choroid

We have previously studied the capability of the micelles to diffuse into and through the sclera in their intact form (Ghezzi et al., 2022). Here, we evaluated the application of the film for 24 hours to confirm its capability to deliver the CYC-loaded nanocarrier to the sclera. The amount of TPGS in the sclera resulted in 78.48 ± 14.90 μg/cm^2, while CYC accumulation was 22.20 ± 6.80 μg/cm^2, which corresponded to a CYC scleral concentration of 150 μg/g (average scleral weight: 149.83 ± 23.37 mg/cm^2). As expected, the accumulation values were lower if compared to the application of a simple micellar solution (Ghezzi et al., 2022), confirming the ability of the platform to control the release of the loaded micelles. The swelling index of the film after the experiment was 19.20 ± 5.82.

Figure 8 reports images and emission spectra acquired on the sclera by two-photon microscopy after the application of blank and NR-loaded films for 4 hours.

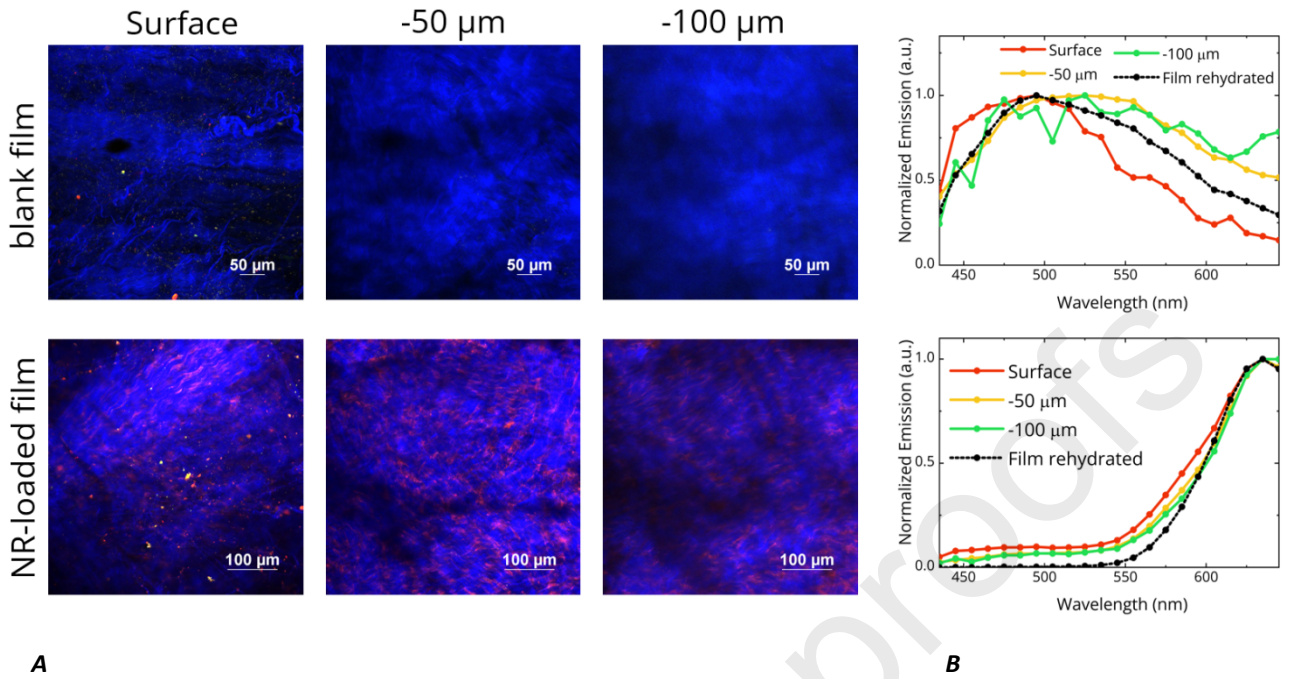

Figure 8. Panel A: TPM images of sclera treated with a blank film or NR-loaded film, acquired after 4h of application. TPM images at three different depths are reported. Panel B: comparison between the emission spectra collected in correspondence of the three TPM images in Panel A. The emission profile of a blank or NR-loaded (rehydrated) film is reported as a comparison. Both images and emission spectra were acquired at 820 nm.

Scleral tissue treated with the blank polymeric films presented a very weak fluorescence signal, which was not visible in the TPM images, but it was characterized by a bandshape almost superimposable to the emission of the rehydrated blank film. In the case of the tissue treated with NR-loaded films, the emission from the dye mainly came from the pores in between the collagen fibers, as already observed for TPGS micelles loaded with NR (Ghezzi et al., 2022). The emission profile collected in this tissue was very similar to the one collected from the corresponding rehydrated film, indicating that the polarity of the environment where NR was located has not significantly changed. The low-wavelength shoulder and the low intensity band at 500 nm were due to the autofluorescence of the tissue and the emission of the blank film, as demonstrated in Figure S6. No significant variations in the emission spectra were observed up to 100 µm from the surface.

To better appreciate the distribution of the dye in the tissue, Z-stacks of the same samples (sclera treated with a blank and a NR-loaded film) were also collected (Figure S7).

After penetration through the scleral tissue, micelles find a further barrier to the retina, which is represented by the bilayer composed of choroid and Bruch's membrane (Figure 5), a thin layer characterized by the presence of melanin. Starting from this observation, a 800 µg/mL CYC micellar solution was applied to the isolated choroid-Bruch's membrane. The applied concentration was approximately 5 times higher for comparison to the one found in the sclera in the previous experiment, but was selected for analytical reasons. TPGS and CYC permeation profiles obtained across choroid are shown in Figure 9, Panel A. The calculated flows were 0.82 ± 0.32 µg/cm^{2}h for

TPGS and 0.12 ± 0.01 µg/cm²h for CYC, while permeability coefficients (calculated between 210 and 300 minutes) were 3.00 (± 1.16) × 10^{-8} cm/s and 4.29 (± 2.93) × 10^{-8} cm/s, respectively.

Two-photon microscopy analysis of choroid was not trivial, due to the strong light absorption and autofluorescence of melanin, elastin fibers (Bruch's membrane) and the presence of red/white blood cells (Han et al., 2007; Lapierre-Landry et al., 2018; Sitiwin et al., 2019). For this reason, it was not possible to obtain reliable information about micelles integrity from NR signal in this tissue. However, when the CYC permeated was plotted as a function of the TPGS permeated (Figure 9, Panel B) a linear relationship (R^2 = 0.92) was found with a slope of 8.1, thus reasonably close to the TPGS/CYC ratio in the film (9.3). These data, albeit characterized by high variability, suggest that micelles mostly permeate intact.

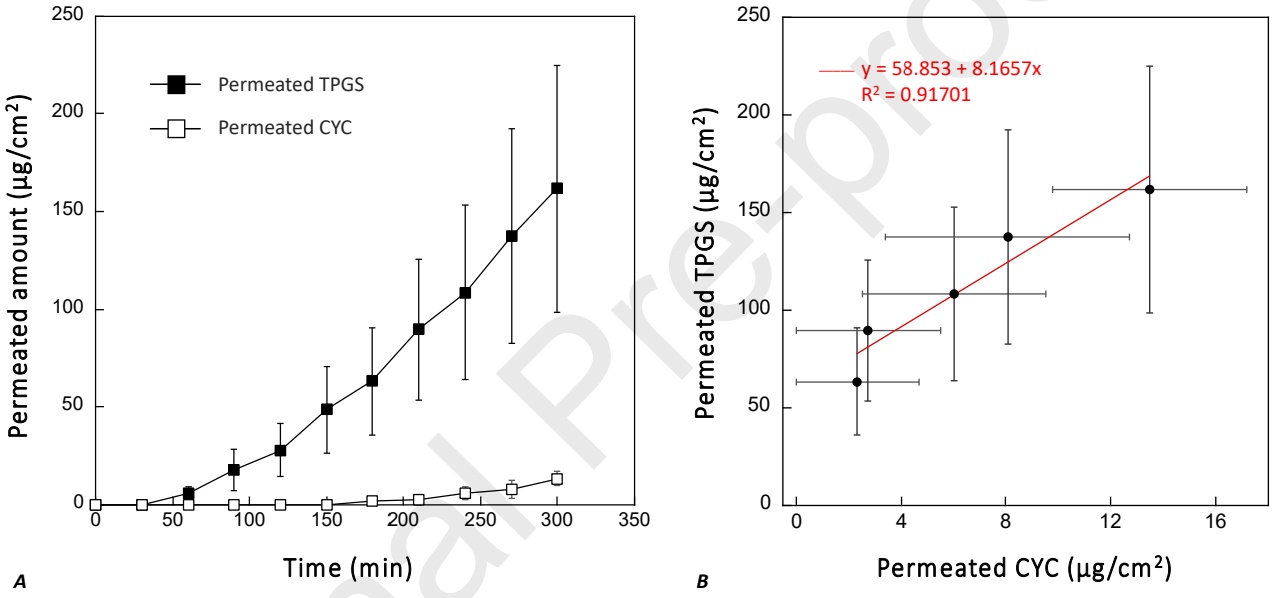

Figure 9. Panel A: amount of TPGS and CYC permeated across choroid (µg/cm²) after the application of a 800 µg/mL CYC micellar solution. Due to the high variability, for the sake of clarity, data are reported as mean ± SEM (n = 4). Panel B: linear relation (R^2 = 0.92) obtained plotting the CYC amount permeated as a function of the TPGS amount permeated (mean ± SEM).

3.5 HET-CAM test

The unloaded and CYC-loaded polymeric platforms, uncrosslinked and crosslinked, were subjected to the HET-CAM test. The chorioallantoic membrane (CAM) of fertilized eggs has a vasculature comparable to the conjunctiva, and therefore, it is considered an alternative to ***in vivo*** testing for evaluating the ocular compatibility of new formulations ("DB-ALM Method Summary n° 96 : Hen's Egg Test on the Chorioallantoic Membrane (HET-CAM) Eye Irritation," n.d.). After 5 minutes in contact with the CAM, no hemorrhage, vascular lysis, or coagulation was observed, so all XG-films (unloaded and loaded) could be considered as nonirritating (Figure S8). Differently, the NaOH solution used as positive control resulted in hemorrhage, vascular lysis, and coagulation showing an irritation score (IS) of 19.85. The IS for the negative control was 0 as for the samples.

3.6 Autoclave crosslinking for simultaneous sterilization

Sterility is a fundamental requirement for ophthalmic formulations and can be achieved with different techniques (Zielińska et al., 2020). Among these, sterilization by moist heat (autoclave) represents the gold standard. In this work, we took advantage of the moist heat sterilization step to simultaneously obtain film crosslinking. For this purpose, samples of the polymeric films were placed in an autoclave at 121 °C for different times, counted starting from the achievement of the useful pressure. The feasibility of this approach was investigated by comparing the swelling behavior of the films.

Figure 10, Panel A compares the swelling profiles of *Formulation A*, that was oven crosslinked at 121 °C for 19 minutes (*Reference formulation*), with the one obtained in the autoclave at 121 °C for 15 minutes, the minimum sterilization conditions required by the European Pharmacopoeia (XII ed.). The obtained results evidenced that the autoclave treatment produces films that swelled less than those processed in the oven because the heat-carrying capacity of steam is much greater than that of air. With the aim to reproduce the reference swelling behavior and given the role of citric acid in the crosslinking (Figure 2, Panel B), we removed this compound from the formulation (*Formulation B*). The data obtained (Figure 10, Panel B) highlighted the possibility of finely tuning the swelling behavior of the films by small variations in the heating time, without the need of using CA to reinforce the crosslinking.

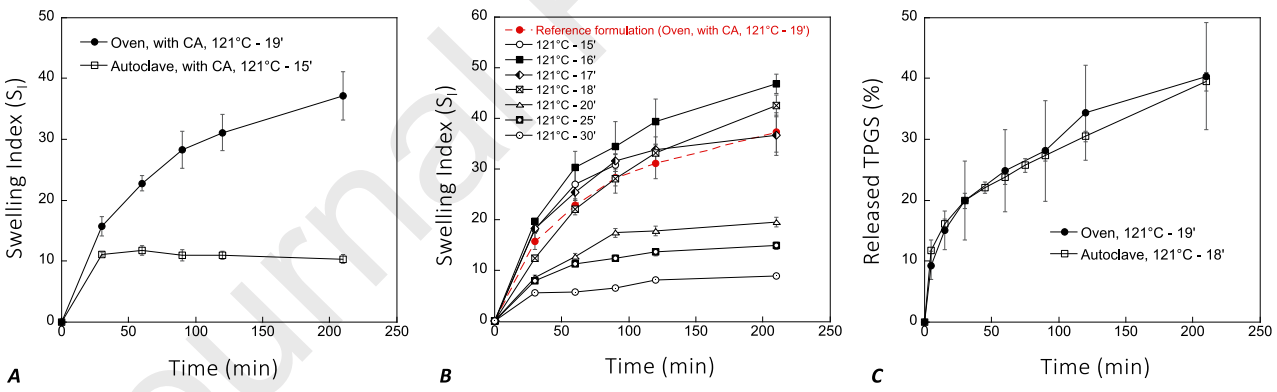

Figure 10. Panel A: comparison between the swelling of the *reference formulation* and the *Formulation A* crosslinked in the autoclave at 121 °C for 15 minutes. Panel B: comparison between the swelling of the *reference formulation* and the *Formulation B* crosslinked in autoclave at 121 °C for different times (in the absence of citric acid). Panel C: comparison between the TPGS release from the *reference formulation* and the *Formulation B* crosslinked in autoclave at 121 °C for 18 minutes. All data are reported as mean ± SD (n = 3).

The film sterilized for 15 minutes did not remain intact, however the progressive increase in heating time was associated with a greater control in the solvent uptake. The condition considered most similar, in terms of film swelling, to the *reference* one was the treatment carried out in the absence of citric acid at 121 °C for 18 minutes. In this condition (121 °C, 18 minutes), the sterility of the film was also assessed by incubating the samples at 37 °C for 10 days in liquid and solid media. The

absence of microbial growth confirmed sterilization efficacy. Images of a film in contact with the solid medium were collected at time points 0 and 10 days (Figures S9).

To confirm that the swelling analogy corresponds to an analogous TPGS release behavior, release studies were carried out. Results (Figure 10, Panel C) highlighted a release profile superimposable with the *Reference formulation*, supporting the one-step crosslinking/sterilization process as a suitable approach for the preparation of sterile, micelles-loaded XG-based films for ocular delivery.

3.7 Mechanical properties of the films

The mechanical properties of the films were strongly dependent on the crosslinking method (Figure 11, Panel A; Figure S10, Panel A in Supplementary Material). Control uncrosslinked films (no-drug loaded) performed as an elastic material, with a relatively low Young's modulus (127.9 MPa), until a 53 % elongation (tensile strain) was achieved (Table 4 and Figure 11, Panel A). Then, plastic deformation continued beyond 120 % elongation. Curing at autoclave (121 °C for 18 minutes) notably reinforced the uniaxial tensile mechanical properties, with an increase in the Young's modulus (196.9 MPa) and the hardness ($\mathbf{F_{max}}$); however, the films became more brittle and the elongation at $\mathbf{F_{max}}$ was of 18.5 %. Crosslinking in the oven of films containing CA increased almost one order of magnitude the Young's modulus values; 939.8 MPa for films crosslinked at 121 °C for 19 minutes and 951.2 MPa for those crosslinked at 130 °C for 90 minutes. These values are among the highest reported ones in literature for polysaccharide-based films; for example, films with thickness (0.1 mm) similar to our formulations made of starch (5 % w/w) dispersions crosslinked with CA (5-30 % with respect to starch) and cured at 150 °C had Young's modulus in between 190 and 1340 MPa (Duarte et al., 2023). In that study, the highest Young's modulus values (and lower elongation at break) corresponded to the films containing the lowest proportion in CA; i.e. 5 and 10 % with respect to starch. In our case, assuming that only XG is efficiently crosslinked by citric acid, the relative proportion of CA was 3 %.

Table 4. Maximum force (F_{max}), elongation at F_{max}, and Young's modulus of the unloaded and drug-loaded films.

FILM	CROSSLINKING CONDITIONS (°C , min)	F_{max} (N)	ELONGATION AT F_{max} (%)	YOUNG´S MODULUS (MPa)
Formulation A, unloaded	Non-crosslinked	21.6	53.0	127.9
Formulation A, unloaded	Oven 121, 19	27.8	13.6	939.8
Formulation A, unloaded	Oven 130, 90	23.9	5.3	951.2
Formulation B, unloaded	Autoclave 121, 18	24.3	18.5	196.9
Formulation A, CYC-loaded	Non-crosslinked	12.2	23.6	266.6
Formulation A, CYC-loaded	Oven 121, 19	25.2	5.4	810.9
Formulation A, CYC-loaded	Oven 130, 90	17.9	4.4	739.2

Incorporation of CYC caused minor changes in the mechanical properties of the films (Table 4 and Figure 11, Panel B). The presence of the drug increased the Young's modulus of uncrosslinked films, probably through hydrophobic interactions with the backbone of the polysaccharide. Differently, a small decrease in Young's modulus was recorded for the films crosslinked in oven at high temperature.

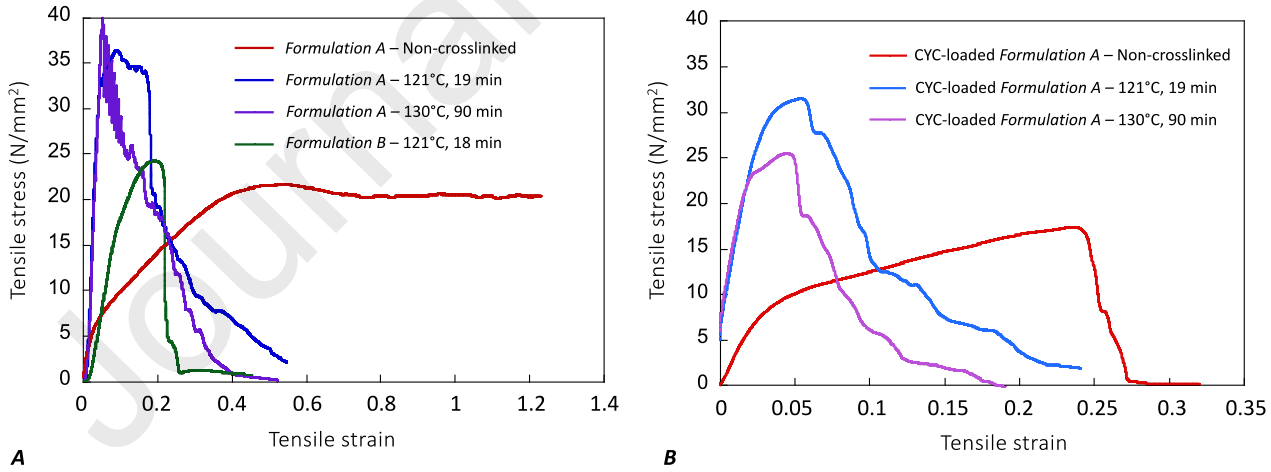

Figure 11. Mechanical profiles recorded for dried films subjected to uniaxial tensile tests. Panel A: unloaded films containing CA (*Formulation A*) that were not crosslinked (thickness: 100 µm), crosslinked in an oven at 121 °C for 19 minutes (thickness: 80 µm) or 130 °C for 90 minutes (thickness: 60 µm), and films crosslinked in an autoclave in the absence of CA (thickness: 100 µm) (*Formulation B*). Panel B: CYC-loaded films (*Formulation A*) not crosslinked (thickness: 70 µm), crosslinked in an oven at 121 °C for 19 minutes (thickness: 80 µm) or 130 °C for 90 minutes (70 µm).

4. Conclusions

The swelling and release data, the ***ex vivo*** studies on ocular tissues, and the microscopic investigations allow to elect the developed XG-based platform as an effective and versatile ocular drug delivery system. **The crosslinked film, in fact, is capable of controlling the release of the loaded TPGS micelles over time, preserving their properties such as the nanometric size, the solubilization capability and the enhanced tissue penetration. Furthermore, the identification of a crosslinking strategy simultaneously with sterilization represents the resolution of a crucial problem for ophthalmic formulations.**

Despite the interesting results, limitations should also be cited: first of all, the potential of this platform is linked to the efficiency of drug encapsulation into the TPGS micelles. Additionally, the potency of the drug should be taken into account, since the need for relatively high amount of TPGS limits the loaded dose. Finally, the stability of the drug under the crosslinking conditions represent a critical aspect and should be carefully evaluated. *In vivo* studies on longer times will be necessary to understand the behaviour of the system in a real in-use environment since film swelling and micelles release could take place with a different kinetic.

Acknowledgments

Authors thank Ferdinando Ruocco and Macello Annoni SpA for kindly providing porcine eye bulbs. Former undergraduate student Francesca Carlomagno is gratefully acknowledged for her contribution in data collection.

Data Statement

The data that support the findings of this study are available from the corresponding author upon reasonable request.

Declaration of Competing Interest

The authors declare that they have no known competing financial interests or personal relationships that could have appeared to influence the work reported in this paper.

REFERENCES

Bhattacharya, S.S., Mishra, A., Pal, D., Ghosh, A.K., Ghosh, A., Banerjee, S., Sen, K.K., 2012. Synthesis and Characterization of Poly(acrylic acid)/Poly(vinyl alcohol)-xanthan Gum Interpenetrating Network (IPN) Superabsorbent Polymeric Composites. Polymer - Plastics Technology and Engineering 51. https://doi.org/10.1080/03602559.2012.671421

Bhunia, T., Giri, A., Nasim, T., Chattopadhyay, D., Bandyopadhyay, A., 2013. Uniquely different PVA-xanthan gum irradiated membranes as transdermal diltiazem delivery device. Carbohydr Polym 95. https://doi.org/10.1016/j.carbpol.2013.02.043

Bi, F., Zhang, X., Liu, Jing, Yong, H., Gao, L., Liu, Jun, 2020. Development of antioxidant and antimicrobial packaging films based on chitosan, D-α-tocopheryl polyethylene glycol 1000 succinate and silicon dioxide nanoparticles. Food Packag Shelf Life 24, 100503. https://doi.org/10.1016/J.FPSL.2020.100503

Boldrini, B., Cavalli, E., Painelli, A., Terenziani, F., 2002. Polar Dyes in Solution: A Joint Experimental and Theoretical Study of Absorption and Emission Band Shapes. https://doi.org/10.1021/jp020031b

Brunchi, C.E., Bercea, M., Morariu, S., Avadanei, M., 2016. Investigations on the interactions between xanthan gum and poly(vinyl alcohol) in solid state and aqueous solutions. Eur Polym J 84. https://doi.org/10.1016/j.eurpolymj.2016.09.006

Bueno, V.B., Bentini, R., Catalani, L.H., Petri, D.F.S., 2013. Synthesis and swelling behavior of xanthan-based hydrogels. Carbohydr Polym 92, 1091–1099. https://doi.org/10.1016/J.CARBPOL.2012.10.062

Cascone, M.G., Sim, B., Sandra, D., 1995. Blends of synthetic and natural polymers as drug delivery systems for growth hormone. Biomaterials 16, 569–574. https://doi.org/10.1016/0142-9612(95)91131-H

Chandra, N.S., Gorantla, S., Priya, S., Singhvi, G., 2022. Insight on updates in polysaccharides for ocular drug delivery. https://doi.org/10.1016/j.carbpol.2022.120014

Cholkar, K., Dasari, S.R., Pal, D., Mitra, A.K., 2013. Eye: anatomy, physiology and barriers to drug delivery. Ocular Transporters and Receptors: Their Role in Drug Delivery 1–36. https://doi.org/10.1533/9781908818317.1

Cortes, H., Caballero-Florán, I.H., Mendoza-Muñoz, N., Escutia-Guadarrama, L., Figueroa-González, G., Reyes-Hernández, O.D., González-Del Carmen, M., Varela-Cardoso, M., González-Torres, M., Florán, B., Del Prado-Audelo, M.L., Leyva-Gómez, G., 2020. Xanthan gum in drug release. Cell Mol Biol 66, 199–207. https://doi.org/10.14715/CMB/2020.66.4.24

DB-ALM Method Summary n° 96 : Hen's Egg Test on the Chorioallantoic Membrane (HET-CAM) Eye Irritation, n.d.

Diaz-Gomez, L., Gonzalez-Prada, I., Millan, R., Da Silva-Candal, A., Bugallo-Casal, A., Campos, F., Concheiro, A., Alvarez-Lorenzo, C., 2022. 3D printed carboxymethyl cellulose scaffolds for autologous growth factors delivery in wound healing. Carbohydr Polym 278, 118924. https://doi.org/10.1016/J.CARBPOL.2021.118924

Diéguez, H.H., González Fleitas, M.F., Aranda, M.L., Calanni, J.S., Keller Sarmiento, M.I., Chianelli, M.S., Alaimo, A., Sande, P.H., Romeo, H.E., Rosenstein, R.E., Dorfman, D., 2020. Melatonin protects the retina from experimental nonexudative age-related macular degeneration in mice. J Pineal Res 68, e12643. https://doi.org/10.1111/JPI.12643

European Parliament, Council, 2010. Directive 2010/63/EU (22 September 2010) on the protection of animals used for scientific purposes. European Union: Brussels, Belgium 1–47.

do Nascimento, F.C., de Aguiar, L.C.V., Costa, L.A.T., Fernandes, M.T., Marassi, R.J., Gomes, A. de S., de Castro, J.A., 2021. Formulation and characterization of crosslinked polyvinyl alcohol

(PVA) membranes: effects of the crosslinking agents. Polymer Bulletin 78, 917–929. https://doi.org/10.1007/S00289-020-03142-2/FIGURES/7

Dong, Y., Zhang, Z., Feng, S.S., 2008. d-α-Tocopheryl polyethylene glycol 1000 succinate (TPGS) modified poly(l-lactide) (PLLA) films for localized delivery of paclitaxel. Int J Pharm 350, 166–171. https://doi.org/10.1016/J.IJPHARM.2007.08.043

Duan, Y., Cai, X., Du, H., Zhai, G., 2015. Novel in situ gel systems based on P123/TPGS mixed micelles and gellan gum for ophthalmic delivery of curcumin. Colloids Surf B Biointerfaces 128, 322–330. https://doi.org/10.1016/j.colsurfb.2015.02.007

Duarte, G.A., Bezerra, M.C., Bettini, S.H.P., Lucas, A.A., 2023. Real-time monitoring of the starch cross-linking with citric acid by chemorheological analysis. Carbohydr Polym 311, 120733. https://doi.org/10.1016/J.CARBPOL.2023.120733

Durgun, M.E., Güngör, S., Özsoy, Y., 2020. Micelles: Promising Ocular Drug Carriers for Anterior and Posterior Segment Diseases. https://home.liebertpub.com/jop 36, 323–341. https://doi.org/10.1089/JOP.2019.0109

El Tayar, N., Mark, A.E., Vallat, P., Brunne, R.M., Testa, B., van Gunsteren, W.F., 1993. Solvent-Dependent Conformation and Hydrogen-Bonding Capacity of Cyclosporin A: Evidence from Partition Coefficients and Molecular Dynamics Simulations. J Med Chem 36. https://doi.org/10.1021/jm00076a002

Ferreira de Melo, I.M., Martins Ferreira, C.G., Lima da Silva Souza, E.H., Almeida, L.L., Bezerra de Sá, F., Cavalcanti Lapa Neto, C.J., Paz de Castro, M.V., Teixeira, V.W., Coelho Teixeira, Á.A., 2020. Melatonin regulates the expression of inflammatory cytokines, VEGF and apoptosis in diabetic retinopathy in rats. Chem Biol Interact 327, 109183. https://doi.org/10.1016/J.CBI.2020.109183

Gabai, A., Zeppieri, M., Finocchio, L., Salati, C., 2023. Innovative Strategies for Drug Delivery to the Ocular Posterior Segment. Pharmaceutics. https://doi.org/10.3390/pharmaceutics15071862

Gautam, L., Warkar, S.G., Ahmad, S.I., Kant, R., Jain, M., 2022. A review on carboxylic acid cross-linked polyvinyl alcohol: Properties and applications. Polym Eng Sci 62, 225–246. https://doi.org/10.1002/PEN.25849

Ghezzi, M., Ferraboschi, I., Delledonne, A., Pescina, S., Padula, C., Santi, P., Sissa, C., Terenziani, F., Nicoli, S., 2022. Cyclosporine-loaded micelles for ocular delivery: Investigating the penetration mechanisms. Journal of Controlled Release 349, 744–755. https://doi.org/10.1016/J.JCONREL.2022.07.019

Ghezzi, M., Pescina, S., Padula, C., Santi, P., Del Favero, E., Cantù, L., Nicoli, S., 2021. Polymeric micelles in drug delivery: An insight of the techniques for their characterization and assessment in biorelevant conditions. Journal of Controlled Release 332, 312–336. https://doi.org/10.1016/J.JCONREL.2021.02.031

Grimaudo, M.A., Pescina, S., Padula, C., Santi, P., Concheiro, A., Alvarez-Lorenzo, C., Nicoli, S., 2019. Topical application of polymeric nanomicelles in ophthalmology: a review on research efforts for the noninvasive delivery of ocular therapeutics. Expert Opin Drug Deliv 16, 397–413. https://doi.org/10.1080/17425247.2019.1597848

Grimaudo, M.A., Pescina, S., Padula, C., Santi, P., Concheiro, A., Alvarez-Lorenzo, C., Nicoli, S., 2018. Poloxamer 407/TPGS Mixed Micelles as Promising Carriers for Cyclosporine Ocular Delivery. Mol Pharm 15, 571–584. https://doi.org/10.1021/ACS.MOLPHARMACEUT.7B00939/ASSET/IMAGES/LARGE/MP-2017-00939B_0009.JPEG

Guo, Y., Luo, J., Tan, S., Otieno, B.O., Zhang, Z., 2013. The applications of Vitamin E TPGS in drug delivery. European Journal of Pharmaceutical Sciences 49, 175–186. https://doi.org/10.1016/J.EJPS.2013.02.006

Han, M., Giese, G., Schmitz-Valckenberg, S., Bindewald-Wittich, A., Holz, F.G., Yu, J., Bille, J.F., Niemz, M.H., 2007. Age-related structural abnormalities in the human retina-choroid complex revealed by two-photon excited autofluorescence imaging. J Biomed Opt 12, 024012. https://doi.org/10.1117/1.2717522

Hardeland, R., Pandi-Perumal, S.R., 2005. Melatonin, a potent agent in antioxidative defense: Actions as a natural food constituent, gastrointestinal factor, drug and prodrug. Nutr Metab (Lond) 2, 22. https://doi.org/10.1186/1743-7075-2-22

Health Organization, W., n.d. World report on vision.

John V. Forrester, Andrew D. Dick, Eric Pearlman, 2016. The Eye. Elsevier. https://doi.org/10.1016/C2012-0-07682-X

Kim, S.Y., Shim, M.S., Kim, K.Y., Weinreb, R.N., Wheeler, L.A., Ju, W.K., 2014. Inhibition of cyclophilin D by cyclosporin A promotes retinal ganglion cell survival by preventing mitochondrial alteration in ischemic injury. Cell Death & Disease 2014 5:3 5, e1105–e1105. https://doi.org/10.1038/cddis.2014.80

Kodavaty, J., 2022. Poly (vinyl alcohol) and hyaluronic acid hydrogels as potential biomaterial systems - A comprehensive review. J Drug Deliv Sci Technol 71, 103298. https://doi.org/10.1016/J.JDDST.2022.103298

Kundeková, B., Máčajová, M., Meta, M., Čavarga, I., Bilčík, B., 2021. Chorioallantoic Membrane Models of Various Avian Species: Differences and Applications. Biology (Basel) 10. https://doi.org/10.3390/BIOLOGY10040301

Lapierre-Landry, M., Carroll, J., Skala, M.C., 2018. Imaging retinal melanin: a review of current technologies. Journal of Biological Engineering 2018 12:1 12, 1–13. https://doi.org/10.1186/S13036-018-0124-5

Li, L., Jin, R., Li, Y., Yoon, H.S., Yoon, H.J., Yoon, K.C., 2021. Effects of eye drops containing a mixture of 3% diquafosol sodium and tocopherol acetate (vitamin E) on the ocular surface of murine dry eye. Cutan Ocul Toxicol 40, 350–358. https://doi.org/10.1080/15569527.2021.1973022

Li, X., Fang, J., Xin, M., Li, Q., Wang, J., Yang, H., Wu, X., 2021. Rebaudioside A/TPGS mixed nanomicelles as promising nanocarriers for nimodipine ocular delivery. Drug Deliv Transl Res 11, 1119–1132. https://doi.org/10.1007/S13346-020-00834-0

Lien, S.M., Ko, L.Y., Huang, T.J., 2009. Effect of pore size on ECM secretion and cell growth in gelatin scaffold for articular cartilage tissue engineering. Acta Biomater 5, 670–679. https://doi.org/10.1016/j.actbio.2008.09.020

Lu, P., Liang, Z., Zhang, Z., Yang, J., Song, F., Zhou, T., Li, J., Zhang, J., 2024. Novel nanomicelle butenafine formulation for ocular drug delivery against fungal keratitis: In Vitro and In Vivo study. Eur J Pharm Sci 192. https://doi.org/10.1016/J.EJPS.2023.106629

Lundmark, P.O., Pandi-Perumal, S.R., Srinivasan, V., Cardinali, D.P., Rosenstein, R.E., 2007. Melatonin in the eye: Implications for glaucoma. Exp Eye Res 84, 1021–1030. https://doi.org/10.1016/J.EXER.2006.10.018

Madni, A., Rahem, M.A., Tahir, N., Sarfraz, M., Jabar, A., Rehman, M., Kashif, P.M., Badshah, S.F., Khan, K.U., Santos, H.A., 2017. Non-invasive strategies for targeting the posterior segment of eye. Int J Pharm 530, 326–345. https://doi.org/10.1016/J.IJPHARM.2017.07.065

Malathi, S., Pavithra, P.S., Sridevi, S., Verma, R.S., 2020. Fabrication of nanopatterned PLGA films of curcumin and TPGS for skin cancer. Int J Pharm 578. https://doi.org/10.1016/J.IJPHARM.2020.119100

Martins, L.G., khalil, N.M., Mainardes, R.M., 2017. Application of a validated HPLC-PDA method for the determination of melatonin content and its release from poly(lactic acid) nanoparticles. J Pharm Anal 7, 388–393. https://doi.org/10.1016/J.JPHA.2017.05.007

Mccusker, M.M., Durrani, K., Payette, M.J., Suchecki, J., 2016. An eye on nutrition: The role of vitamins, essential fatty acids, and antioxidants in age-related macular degeneration, dry eye syndrome, and cataract. https://doi.org/10.1016/j.clindermatol.2015.11.009

Mehata, A.K., Setia, A., Vikas, Malik, A.K., Hassani, R., Dailah, H.G., Alhazmi, H.A., Albarraq, A.A., Mohan, S., Muthu, M.S., 2023. Vitamin E TPGS-Based Nanomedicine, Nanotheranostics, and Targeted Drug Delivery: Past, Present, and Future. Pharmaceutics 15, 722. https://doi.org/10.3390/PHARMACEUTICS15030722

Nayak, K., Misra, M., 2018. A review on recent drug delivery systems for posterior segment of eye. Biomed Pharmacother 107, 1564–1582. https://doi.org/10.1016/J.BIOPHA.2018.08.138

Nsengiyumva, E.M., Alexandridis, P., 2022. Xanthan gum in aqueous solutions: Fundamentals and applications. Int J Biol Macromol 216, 583–604. https://doi.org/10.1016/J.IJBIOMAC.2022.06.189

Ostacolo, C., Caruso, C., Tronino, D., Troisi, S., Laneri, S., Pacente, L., Del Prete, A., Sacchi, A., 2013. Enhancement of corneal permeation of riboflavin-5'-phosphate through vitamin E TPGS: A promising approach in corneal trans-epithelial cross linking treatment. Int J Pharm 440, 148–153. https://doi.org/10.1016/J.IJPHARM.2012.09.051

Pahuja, P., Arora, S., Pawar, P., 2012. Ocular drug delivery system: a reference to natural polymers. Expert Opin Drug Deliv 9, 837–861. https://doi.org/10.1517/17425247.2012.690733

Pardue, M.T., Allen, R.S., 2018. Neuroprotective strategies for retinal disease. Prog Retin Eye Res 65, 50–76. https://doi.org/10.1016/J.PRETEYERES.2018.02.002

Pescina, S., Lucca, L.G., Govoni, P., Padula, C., Del Favero, E., Cantù, L., Santi, P., Nicoli, S., 2019. Ex Vivo Conjunctival Retention and Transconjunctival Transport of Poorly Soluble Drugs Using Polymeric Micelles. Pharmaceutics 11. https://doi.org/10.3390/PHARMACEUTICS11090476

Pescina, S., Santi, P., Ferrari, G., Padula, C., Cavallini, P., Govoni, P., Nicoli, S., 2012. Ex vivo models to evaluate the role of ocular melanin in trans-scleral drug delivery. Eur J Pharm Sci 46, 475–483. https://doi.org/10.1016/J.EJPS.2012.03.013

Pescina, S., Sonvico, F., Clementino, A., Padula, C., Santi, P., Nicoli, S., 2021. Preliminary investigation on simvastatin-loaded polymeric micelles in view of the treatment of the back of the eye. Pharmaceutics 13, 855. https://doi.org/10.3390/PHARMACEUTICS13060855/S1

Polisetti, N., Martin, G., Cristina Schmitz, H.R., Schlötzer-Schrehardt, U., Schlunck, G., Reinhard, T., 2023. Characterization of Porcine Ocular Surface Epithelial Microenvironment. Int J Mol Sci 24, 7543. https://doi.org/10.3390/IJMS24087543/S1

Qi, Q., Wei, Y., Zhang, X., Guan, J., Mao, S., 2023. Challenges and strategies for ocular posterior diseases therapy via non-invasive advanced drug delivery. Journal of Controlled Release 361, 191–211. https://doi.org/10.1016/J.JCONREL.2023.07.055

Rathod, S., Bahadur, P., Tiwari, S., 2021. Nanocarriers based on vitamin E-TPGS: Design principle and molecular insights into improving the efficacy of anticancer drugs. Int J Pharm 592. https://doi.org/10.1016/J.IJPHARM.2020.120045

Ray, S., Banerjee, S., Maiti, S., Laha, B., Barik, S., Sa, B., Bhattacharyya, U.K., 2010. Novel interpenetrating network microspheres of xanthan gumpoly(vinyl alcohol) for the delivery of diclofenac sodium to the intestinein vitro and in vivo evaluation. Drug Deliv 17. https://doi.org/10.3109/10717544.2010.483256

Reddy, N., Yang, Y., 2010. Citric acid cross-linking of starch films. Food Chem 118, 702–711. https://doi.org/10.1016/J.FOODCHEM.2009.05.050

Repka, M.A., McGinity, J.W., 2001. Bioadhesive properties of hydroxypropylcellulose topical films produced by hot-melt extrusion. Journal of Controlled Release 70, 341–351. https://doi.org/10.1016/S0168-3659(00)00365-5

Rodrigues, G.A., Lutz, D., Shen, J., Yuan, X., Shen, H., Cunningham, J., Rivers, H.M., 2018. Topical Drug Delivery to the Posterior Segment of the Eye: Addressing the Challenge of Preclinical to Clinical Translation. Pharm Res 35. https://doi.org/10.1007/S11095-018-2519-X

Ruiz, F., Alvarez, G., Ramos, M., Hernández, M., Bogónez, E., Satrústegui, J., 2000. Cyclosporin A targets involved in protection against glutamate excitotoxicity. Eur J Pharmacol 404, 29–39. https://doi.org/10.1016/S0014-2999(00)00584-7

Sande, P.H., Dorfman, D., Fernandez, D.C., Chianelli, M., Domínguez Rubio, A.P., Franchi, A.M., Silberman, D.M., Rosenstein, R.E., Sáenz, D.A., 2014. Treatment with melatonin after onset of experimental uveitis attenuates ocular inflammation. Br J Pharmacol 171, 5696–5707. https://doi.org/10.1111/BPH.12873

Schnichels, S., Schultheiss, M., Klemm, P., Blak, M., Herrmann, T., Melchinger, M., Bartz-schmidt, K.U., Löscher, M., Zeck, G., Spitzer, M.S., Hurst, J., 2021. Cyclosporine A Protects Retinal Explants against Hypoxia. International Journal of Molecular Sciences 2021, Vol. 22, Page 10196 22, 10196. https://doi.org/10.3390/IJMS221910196

Shijie Xu, Zhang, P., Ma, W., Yang, H., Cao, Z., Gong, F., Zhong, J., 2022. High Water Resistance Polyvinyl Alcohol Hydrogel Film Prepared by Melting Process Combining with Citric Acid Cross-Linking. Polymer Science - Series B 64, 198–208. https://doi.org/10.1134/S1560090422020130

Sitiwin, E., Madigan, M.C., Gratton, E., Cherepanoff, S., Conway, R.M., Whan, R., Macmillan, A., 2019. Shedding light on melanins within in situ human eye melanocytes using 2-photon microscopy profiling techniques. Scientific Reports 2019 9:1 9, 1–18. https://doi.org/10.1038/s41598-019-54871-y

Terreni, E., Chetoni, P., Burgalassi, S., Tampucci, S., Zucchetti, E., Chipala, E., Alany, R.G., Al-Kinani, A.A., Monti, D., 2021a. A hybrid ocular delivery system of cyclosporine-A comprising nanomicelle-laden polymeric inserts with improved efficacy and tolerability. Biomater Sci 9, 8235–8248. https://doi.org/10.1039/D1BM01453F

Terreni, E., Chetoni, P., Tampucci, S., Burgalassi, S., Al-Kinani, A.A., Alany, R.G., Monti, D., 2020. Assembling Surfactants-Mucoadhesive Polymer Nanomicelles (ASMP-Nano) for Ocular Delivery of Cyclosporine-A. Pharmaceutics 12. https://doi.org/10.3390/PHARMACEUTICS12030253

Terreni, E., Zucchetti, E., Tampucci, S., Burgalassi, S., Monti, D., Chetoni, P., 2021b. Combination of Nanomicellar Technology and In Situ Gelling Polymer as Ocular Drug Delivery System (ODDS) for Cyclosporine-A. Pharmaceutics 13, 1–28. https://doi.org/10.3390/PHARMACEUTICS13020192

Thrimawithana, T.R., Young, S., Bunt, C.R., Green, C., Alany, R.G., 2011. Drug delivery to the posterior segment of the eye. Drug Discov Today 16, 270–277. https://doi.org/10.1016/J.DRUDIS.2010.12.004

Vaneev, A., Tikhomirova, V., Chesnokova, N., Popova, E., Beznos, O., Kost, O., Klyachko, N., 2021. Nanotechnology for Topical Drug Delivery to the Anterior Segment of the Eye. Int J Mol Sci 22, 22. https://doi.org/10.3390/IJMS222212368

Vivero-Lopez, M., Sparacino, C., Quelle-Regaldie, A., Sánchez, L., Candal, E., Barreiro-Iglesias, A., Huete-Toral, F., Carracedo, G., Otero, A., Concheiro, A., Alvarez-Lorenzo, C., 2022. Pluronic®/casein micelles for ophthalmic delivery of resveratrol: In vitro, ex vivo, and in vivo tests. Int J Pharm 628, 122281. https://doi.org/10.1016/J.IJPHARM.2022.122281

Vuddanda, P.R., Montenegro-Nicolini, M., Morales, J.O., Velaga, S., 2017. Effect of plasticizers on the physico-mechanical properties of pullulan based pharmaceutical oral films. Eur J Pharm Sci 96, 290–298. https://doi.org/10.1016/J.EJPS.2016.09.011

Wang, C., An, Y., Xia, Z., Zhou, X., Li, H., Song, S., Ding, L., Xia, X., 2022. The neuroprotective effect of melatonin in glutamate excitotoxicity of R28 cells and mouse retinal ganglion cells. Front Endocrinol (Lausanne) 13. https://doi.org/10.3389/FENDO.2022.986131

Wang, J., Li, M., Geng, Z., Khattak, S., Ji, X., Wu, D., Dang, Y., 2022. Role of Oxidative Stress in Retinal Disease and the Early Intervention Strategies: A Review. Oxid Med Cell Longev 2022. https://doi.org/10.1155/2022/7836828

Wong, 2009. Composition and method for treating dry eye syndrome. Invest. Ophthalmol. Visual Sci 15, 11–16.

Yang, C., Wu, T., Qi, Y., Zhang, Z., 2018. Recent Advances in the Application of Vitamin E TPGS for Drug Delivery. Theranostics 8, 464. https://doi.org/10.7150/THNO.22711

Yu, H., Wang, Q., Wu, W., Zeng, W., Feng, Y., 2021. Therapeutic Effects of Melatonin on Ocular Diseases: Knowledge Map and Perspective. Front Pharmacol 12. https://doi.org/10.3389/FPHAR.2021.721869/FULL

Zhang, F., Lin, B., Huang, S., Wu, P., Zhou, M., Zhao, J., Hei, X., Ke, Y., Zhang, Y., Huang, D., 2023. Melatonin Alleviates Retinal Ischemia-Reperfusion Injury by Inhibiting p53-Mediated Ferroptosis. Antioxidants (Basel) 12. https://doi.org/10.3390/ANTIOX12061173

Zielińska, A., Soles, B.B., Lopes, A.R., Vaz, B.F., Rodrigues, C.M., Alves, T.F.R., Klensporf-Pawlik, D., Durazzo, A., Lucarini, M., Severino, P., Santini, A., Chaud, M. V., Souto, E.B., 2020. Nanopharmaceuticals for Eye Administration: Sterilization, Depyrogenation and Clinical Applications. Biology 2020, Vol. 9, Page 336 9, 336. https://doi.org/10.3390/BIOLOGY9100336

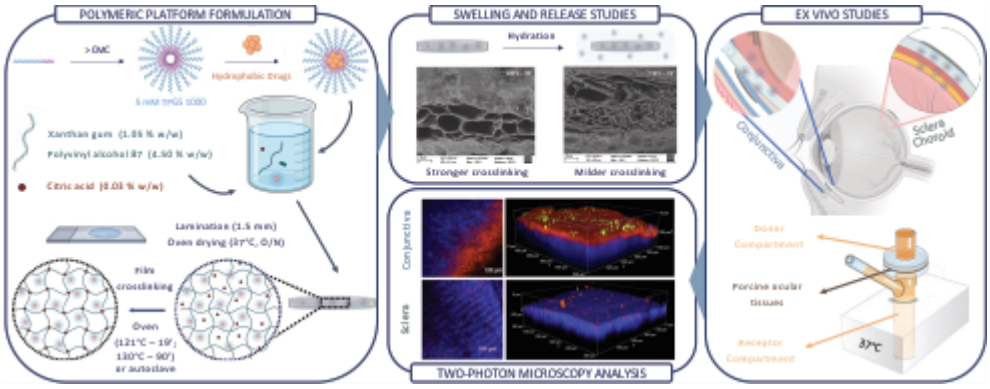

Declaration of interests

☒ The authors declare that they have no known competing financial interests or personal relationships that could have appeared to influence the work reported in this paper.

☐ The authors declare the following financial interests/personal relationships which may be considered as potential competing interests: